Chapter 7

AVIATION IMPACT ON ATMOSPHERIC COMPOSITION AND CLIMATE

U. Schumann and J. Ström

Contributing Authors
F. Arnold, T.K. Berntsen, P.M. de F. Forster, J.-F. Gayet and D. Hauglustaine

HIGHLIGHTS

- Significant improvement has been achieved in recent years in the quantitative understanding of how aircraft emissions change the atmospheric abundances of gases and particles and form contrails. Both soot and volatile particles contribute nuclei for the formation of contrails and cirrus particles. Measurements have confirmed that aircraft exhaust plumes contain H_2SO_4. The efficiency of fuel sulphur conversion to H_2SO_4 amounts to ε=3.3±1.8% based on these measurements, less than what was expected from indirect estimates. The value of ε is engine dependent. The number of Chemiions (CIs) mainly controls the number of volatile particles formed in exhaust plumes. The size of the particles in the plume depends on the abundance of sulphuric acid and organic acids. CIs contain sulphur-bearing molecules and organics. Soot particles contribute to contrail crystal nucleation. The number of volatile particles produced in aircraft plumes is of the order 10^{17} per kg of burned fuel and is about 100-1000 times larger than the number of soot particles emitted. On average the global subsonic fleet emits 0.04 g soot per kg of fuel. Nitric acid is of small importance for aerosol formation in aircraft wakes under typical tropopause conditions.

- Recent models compute much smaller radiative forcing (RF) by line-shaped contrails than reported in IPCC [1999]. For about 15% of their flight time, subsonic airliners fly in air masses that are supersaturated with respect to the ice phase in the upper troposphere, and occasionally even in the lowermost stratosphere. The ice supersaturation is often large enough to let contrails develop into cirrus but not large enough to let cirrus clouds form naturally. Operational models do not describe ice supersaturation hence the effect is not modelled. The annual mean contrail cover over Europe is smaller than predicted in previous calculations. The optical depth of contrails over Europe is about 0.06-0.2 and hence smaller than assumed in the past (0.3). It has been experimentally confirmed that more fuel-efficient engines cause contrails to form at higher ambient temperatures. A future climate (with a warmer upper troposphere) shows a lesser tendency to form contrails. A fleet of cryogenic aircraft would give rise to 50% more contrails, but these contrails would be optically thinner than those produced by conventional aircraft. The indirect effects of contrails and aerosols from aircraft on cirrus clouds are still not quantified. In air masses with high soot concentration, cirrus particles are smaller. Progress in assessing aircraft induced changes in cirrus cloudiness has still to come from ongoing and future projects.

- Regional enhancements of nitrogen oxides and aerosols due to aviation emissions at scales up to 1000 km have been measured. Near the tropopause in the range of aviation cruise altitudes over the North Atlantic in the summer, the NO_x concentrations are of the order 0.1 nmol/mol, higher than expected in early studies of aviation impact. Lightning

contributes less than aviation to NO_x sources in the upper troposphere over Europe. The opposite is true for the global mean where lightning is more important.

- The ozone production in the upper troposphere and lower stratosphere increases with NO_x emissions by aviation. Acetone and other carbonyls enhance the ozone production induced by aircraft NO_x. The NO_x impact on ozone is 10-30% smaller than computed previously because of plume processing. Coupled climate/chemistry models show a reduced NO_x-impact on O_3 chemistry in a future climate. The feedback of NO_x on methane may be smaller than assumed before. Aircraft emissions may contribute to some reduction of ozone by heterogeneous chemistry in the lowermost stratosphere, but direct evidence for this effect is missing. Recent studies confirm that aviation presently does not increase UV radiation at the surface.

- The accumulation of carbon dioxide (CO_2) emissions by aircraft until 2000 have contributed to climate change through an increase in RF by nearly 2% compared to the RF from all anthropogenic CO_2 emissions. The CO_2 emissions were increasing at a rate of about 3% per year in the last two decades.

7.1 INTRODUCTION

Aircraft emissions are considered because of their potential impact on the ozone layer, on climate, and on regional air pollution. Aircraft emit gases, particles, and ions into the atmosphere mainly in the upper troposphere and lower stratosphere. Presently these emissions occur primarily in northern hemisphere mid-latitudes. They alter the concentration of greenhouse gases, including carbon dioxide (CO_2), water vapour (H_2O), ozone (O_3) and methane (CH_4). Aircraft emissions trigger formation of condensation trails (contrails) and may increase cirrus cover or change other cloud properties, all of which affect the energy and water budgets of the atmosphere and hence may contribute to climate change at the regional and global scale. Aircraft emissions, at least from supersonic aircraft flying in the stratosphere, may change the ozone layer and the UV radiation at the Earth surface. Aircraft add to nitrogen oxides (NO_x), carbon monoxide (CO), hydrocarbons, and particulate matter near airports and may contribute to local ozone changes.

The environmental impact of aviation has been studied with respect to noise and local air pollution in the neighbourhood of airports since about 1960. The impact of emissions of supersonic aircraft on stratospheric ozone depletion has been studied since about 1970. The impact of the emissions of the world-wide subsonic aviation on ozone formation in the tropopause region and climate has been studied since about 1990. This review considers mainly the possible impact on ozone and climate.

Because of the importance of aviation, its potential impact on the environment, the potential economic consequences, and the large uncertainties of previous assessments, several research programs have been initiated over the last decade, dealing with the impact of aircraft emissions on the atmosphere. In 1991, the German Science Foundation (DFG) initiated basic research on the impact of aircraft and spacecraft emissions on the atmosphere [Schumann, 1998], and several other national programmes followed. In 1992, the EC started the AERONOX project, and several further research programs were launched thereafter, see Table 7.1. In the USA, NASA performed a High Speed Civil Transport (HSCT) research programme (1990-1999), and later a subsonic aviation assessment programme (SASS, 1993-2000) [Kawa et al., 1999; Friedl, 1997]. Research on the environmental aspects of air traffic and operation, fuel and engine

performance, is coordinated within the AERONET network [Dewes et al., 2000]. Coordination of EC and nationally funded projects aimed at improving predictions of aviation induced future changes in climate and stratospheric ozone depletion occurs within the CORSAIRE cluster. Ongoing projects dealing specifically with aviation impact include the EU projects CRYOPLANE, TRADEOFF, INCA, and PARTEMIS, the German project PAZI, and two projects within the UK "Upper Troposphere Lower Stratosphere (UTLS) Ozone" programme ([Law and Penkett, 2000]; http://utls.nerc.ac.uk/), see Table 7.1.

The results of these studies have been periodically reviewed in scientific journals and international assessments [Schumann, 1994, 1997a; WMO, 1995; Fabian and Kärcher, 1997; EU, 1998; IPCC, 1999]. The European Scientific Assessment of the Atmospheric Effects of Aircraft Emissions [EU, 1998] was an important precursor to the Special Report of the Intergovernmental Panel on Climate Change (IPCC) on "Aviation and the Global Atmosphere" [IPCC, 1999], where European research and scientists made significant contributions. The present chapter summarises the major findings from these assessments and reviews the progress reached until end of the year 2000.

The gases and particles emitted or formed as a result of aviation may have an impact on climate both directly and indirectly. The direct effect is due to absorption and scattering of radiation. Indirect effects on climate are many and result from chemical and physical interactions by aircraft emissions on gases, particles and clouds. The IPCC report states that the disturbances induced by global aviation caused an additional radiative forcing (heating) of the Earth-atmosphere system by aircraft of about 0.05 Wm^{-2} or approximately 3.5% (without forcing from cirrus perturbations) of the total RF by all anthropogenic activities in 1992. The disturbances are presently increasing with time both in absolute and relative terms. Nitrogen oxides (NO_x) emissions from current aircraft are calculated to have increased O_3 by about 6% in the region 30-60°N latitude and 9-13 km altitude. Calculated changes in the total column of O_3 in this latitude range are approximately 0.4%. Calculated effects are substantially smaller outside this region. Emissions of NO_x into the stratosphere above about 20km might cause a reduction of ozone. An order of 1% reduction of stratospheric O_3 column and a corresponding increase of UV radiation at the surface may occur if a large (1000 aircraft) fleet of supersonic aircraft would become operational [IPCC, 1999].

Recent assessments [EU, 1998; IPCC, 1999] concluded their reports by identifying open questions that require urgent attention in order to increase our understanding required for assessing aviation impact on the global atmosphere. Common to both reports are the following questions 2, 3, 5. The IPCC report also identifies question 4, and the European assessment includes question 1:

1. What is the precise composition of the aircraft emissions and what is their role in aerosol particle formation?

2. How do contrails and aerosols influence cirrus clouds and chemical processes?

3. What is the mechanism for vertical and horizontal transports of gases and particles in the upper troposphere and lower stratosphere?

4. What is the role of nitrogen oxides in changing the ozone and methane concentration?

5. What are the effects of aircraft on climate?

This Chapter first summarises (in Section 7.2) the results from the previous assessments, and then discusses (in Section 7.3) the advances made in our knowledge with respect to the questions stated above. Section 7.2 summarises the state of the art with general reference to IPCC [1999] unless stated otherwise.

Since the publication of the EU assessment in 1998 [Brasseur et al., 1998] and the IPCC report in 1999, several European and national projects have enhanced the level of scientific understanding of the atmospheric impacts by aviation. Highlights of the new research, with strong contributions from European groups, are mentioned below. The quantification of changes in cirrus properties caused by air traffic remains the key uncertainty in assessing the aviation impact on climate.

7.2 THE PROBLEM AND THE GENERAL ASSESSMENT

Traffic

In 1999, more than 14000 jet, 3400 turbo-prop, and 350 piston-engine commercial aircraft carried 1.6×10^9 revenue passengers world-wide, on average over a distance of 1800 km per flight (data from the International Civil Aviation Organisation, Montreal, 2000). In the period 1981-1999 passenger traffic increased by 5.2% yr^{-1} from 1100 to 2800×10^9 revenue passenger-kilometres, and freight traffic by 7.2% yr^{-1} from 31 to 110×10^9 freight tonne-kilometres per year. For the future, global passenger air travel may continue to grow by about 5% yr^{-1} in terms of revenue passenger-kilometres. The IPCC [1999] assessment considered scenarios with traffic increases by factors from 3 to more than 10 in the year 2050 relative to 1992.

Fuel Consumption

According to IPCC [1999], various inventory calculations (named in brackets) resulted in total fuel use by aviation in 1992 of 129 Tg (DLR), 131 Tg (ANCAT), and 139 Tg (NASA). Several simplifying assumptions in these inventory calculations were identified which caused a systematic underestimate of fuel burned by aviation on the order of 15%. Therefore the values used for the radiative forcing assessments in that study were scaled by a factor 1.15, implying a range from 149 to 160 Tg for 1992. Recent studies give reasons which corroborate the validity of the larger estimate [Daggett et al., 1999]; fuel use reported by American airlines was 17% higher than expected from the NASA inventory. The International Energy Agency [IEA, 2000] reports an aviation fuel refinery output of 165 Tg fuel/yr for 1992 (171 for 1990). The differences between the IEA value and the various inventory values amount to 3-10%. A thorough error analysis of the IEA-data is missing, and the IEA values may overestimate the actual use of fuels for aviation, because a small fraction of the production is used for other purposes [IPCC, 1999]. Since the IEA values become available regularly every year, they may be used as best-estimates of the real fuel consumption and their trends, with an uncertainty of less than 10%. The military fraction for 1992 was estimated in the IPCC report to amount to about 18%. The International Energy Agency reports aviation fuel production values, which grew by about 2.6% annually from 127 to 196 Tg yr^{-1} from 1981 to 1998, and may have exceeded 200 Tg yr^{-1} and even reached 220 Tg yr^{-1} in the year 2000. This extrapolation is supported by data given by the Department of Energy of the USA (see Table 7.2). About 65% of the fuel is consumed at cruise altitudes between 10 and 13 km and most of the emissions occur between 30 and 55°N over the USA, Europe, and the North Atlantic [IPCC, 1999]. The

day/night ratio of fuel consumption amounts to about 3 globally. Averaged over the globe, an estimated 30% of the fuel is consumed in the stratosphere. In the future, total aviation fuel use may grow slightly faster than before, by about 3-4% yr^{-1} between 1990 and 2015 because a reduced military fraction can no longer balance the increasing civil fraction, and because efficiency increases are becoming more difficult to realise in the already quite advanced aviation technology.

Emissions

When burning kerosene with air in the combustion chamber (combustor) of the aircraft engine, a number of species are formed of relevance to atmospheric chemistry and of environmental concern. Carbon dioxide (CO_2) and water vapour (H_2O) dominate the exhaust. Other gaseous emissions are nitrogen oxides (NO_x), hydrocarbons (HC), carbon monoxide (CO), and sulphur oxides (SO_x). Particulate emissions are primarily in the form of soot, condensed vapours, and chemiions (see below). Emission indices, in grams of species formed per kilogram fuel burned, are summarised in Table 7.2.

Aircraft emissions of CO and hydrocarbons are much smaller in amount than other anthropogenic emissions and of little importance for air chemistry outside airports. Methane (CH_4) concentrations at engine exit may even be smaller than in the ambient air. Because of higher combustion temperature and pressure in more fuel-efficient modern engines, total aviation NO_x emissions increased faster than fuel consumption over recent decades. Per unit of fuel consumption the emission masses of CO and HC have decreased [IPCC, 1999].

Changes in Air Composition

Accumulation of aircraft emitted nitrogen oxides and particles have been measured regionally near main traffic corridors at least under low wind conditions during POLINAT (see below). Emissions into the lowermost stratosphere, just above the tropopause are mixed zonally and north- and southward, and leave the stratosphere by stratosphere-troposphere exchange processes mainly on surfaces of constant potential temperature connecting the mid-latitude lower stratosphere with the upper tropical troposphere [e.g., Schoeberl and Morris, 2000]. Inert emissions reside for several weeks to months in the lower stratosphere and a few weeks in the upper troposphere. Nitrogen oxides are converted to nitric acid within a few days. Numerical simulations imply an increase in zonally averaged NO_x from aircraft by about 30% in summer and 60% in winter near the tropopause at northern mid-latitudes [IPCC, 1999].

Carbon Dioxide

Because of its long lifetime, the effects of CO_2 emissions from aircraft are indistinguishable from the same quantity of CO_2 emitted at the same time by any other source in the lower atmosphere. By 2000, the atmospheric CO_2 concentration reached 367 $\mu mol\ mol^{-1}$, about 86 $\mu mol\ mol^{-1}$ more than in 1850, and is responsible for a RF of about 1.5 Wm^{-2} [IPCC, 1996, 2001; Myhre et al., 1998b]. For an order of magnitude estimate one assumes that 1 Wm^{-2} RF causes a global change in surface temperature of the order of 0.4-1.0 K [Cess et al., 1989; Christiansen, 1999].

Past emissions from aviation caused a CO_2 increase of less than 1.7 $\mu mol\ mol^{-1}$ in 2000, i.e., less than 2% of the total increase [Sausen and Schumann, 2000]. Because aviation emissions

have mainly occurred in the last 50 years, this percentage is lower than aviation's present share of the current total CO_2 emissions, which is close to 2.7%. Aviation contributes presently to about 13% of traffic-originating CO_2 emissions [IPCC, 1999]. The aviation share in CO_2 emissions is likely to increase if other CO_2 emissions are reduced [Lee and Sausen, 2000].

Ozone

Tropospheric ozone has increased at northern midlatitudes by about 50% over the past hundrend years as a result of the sum of all anthropogenic sources of NO_x, CO, CH_4, and other hydrocarbons [Lelieveld, and Dentener, 2000]. Stratospheric ozone values have decreased globally. An annual mean value of -2% per decade has been detected for the mid- and low-latitudes (60°S-60°N). A stronger decrease has been found during spring-time in the Arctic and Antarctic lower stratosphere, i.e., -6% per decade and -20% per decade, respectively [WMO, 1999].

NO_x emissions from the present fleet of subsonic aircraft, flying essentially below 13 km altitude, cause O_3 increases, while the same emissions from a potential future fleet of supersonic aircraft may cause O_3 destruction if flying above at least 16 km. Because of long NO_x and O_3 lifetimes, the O_3 changes occur at far distances from the aircraft routes. Because of longer residence time of NO_x, the number of O_3 molecules formed per additional NO_x molecule is higher in the upper troposphere than near the surface. Increases in O_3 in the cold upper troposphere are more effective in increasing RF than increases at lower altitudes [IPCC, 1999].

The NO_x emissions from subsonic aircraft in 1992 are estimated to have increased O_3 concentrations at cruise altitudes in northern mid-latitudes and polar regions by up to 6%, compared to an atmosphere without aircraft emissions. This change in O_3 concentration is of similar magnitude to the natural year to year variability. The impact on O_3 concentrations in other regions of the world is substantially less. Due to the greenhouse effect of O_3, these increases tend to warm the Earth's surface. Moreover, the increased O_3 concentration causes a slight decrease of UV radiation at the Earth's surface. According to calculations, aviation added 0.4% to the total O_3 column in 1992. The erythemal dose rate (UV irradiance causing sunburn, see Chapter 6) is estimated to have been decreased by aircraft in 1992 by about 0.5% at 45°N in July. The aircraft effect on UV is small compared to that caused by other O_3 changes [IPCC, 1999].

Methane

Direct contributions from aircraft emissions to methane are unimportant, but through enhancement of NO_x in the upper troposphere aircraft emissions may indirectly lead to reductions of CH_4. An increase in NO_x leads to an increase of hydroxyl radicals (OH), which in turn leads to an increased destruction of CH_4. The global CH_4 concentration in 1992 has been estimated to be about 2% less than that in an atmosphere without aircraft [IPCC, 1999], but this value is very uncertain (see below).

Water Vapour

The amount of H_2O emitted by aviation is much smaller than the amount of water evaporating at the Earth's surface but comparable in magnitude to the amount of water resulting from CH_4

oxidation in the stratosphere. About 60-70% of subsonic aircraft H_2O emissions are released in the troposphere and removed by precipitation within 1-3 weeks. The remaining fraction of H_2O emissions is released in the lower stratosphere where background concentrations are smaller, residence times longer (on order of a few months), and where H_2O can build up to larger concentrations. Because H_2O is a greenhouse gas, these increases tend to warm the Earth's surface. Additional H_2O in the stratosphere may also produce hydroxyl radicals and reduce O_3 directly, or indirectly by forming polar stratospheric clouds, which cause halogen activation. However, for subsonic aircraft these effects are small compared to the other climatic or chemical effects of aircraft emissions [IPCC, 1999].

Aerosols

Aircraft engines emit soot particles, metal particles, water vapour, chemiions, sulphuric acid, sulphuric acid precursors, and organic gases. CIs are electrically charged molecular clusters [Arnold et al., 1999]. In the plume many new liquid particles are formed mainly by chemiion-induced nucleation of condensable species. CIs enhance the nucleation and coagulation frequency by electrostatic forces. Part of the gases and small new particles may be adsorbed on the surfaces of soot and (a few) metal particles and form a liquid coating. The emitted and freshly formed particles and gases interact with each other and with the particles and gases entrained from ambient air during the mixing process. They grow in size by coagulation and by further uptake of condensable gases. The water containing liquid particles freezes when large, diluted, and cold enough. The resultant aerosol contains a mixture of volatile and non-volatile materials. The volatile material disappears in particle counters when the aerosol is heated to a temperature of about 120°C or more [IPCC, 1999].

With respect to particle characteristics in the plume the conversion of fuel sulphur to sulphuric acid (H_2SO_4) in the exhaust is important. Fuel contains on average about 400 (1-3000) µg/g of sulphur. Most of the fuel sulphur is burned to sulphur dioxide (SO_2) in the combustion chamber of the engine. A fraction is oxidised by reactions with co-emitted hydroxyl radicals (OH) and water to S^{VI} in form of sulphur trioxide (SO_3) and sulphuric acid (H_2SO_4). The H_2SO_4 contributes to particle formation in the exhaust plume [IPCC, 1999].

Subsonic aircraft emissions are a significant source of soot and sulphate aerosol concentrations near the tropopause at northern mid-latitudes, at least by number [IPCC, 1999]. Around 10^{15} soot particles, typical diameters of 30-60 nm, and more than 10^{17} small liquid particles, typical diameters of 2-10 nm, are formed in the exhaust plume per kg of burnt fuel. The resultant number density of soot particles in the exhaust gases at engine exit exceeds 10^6 cm^{-3}; for comparison, the number density of aerosols of the same size in the ambient upper troposphere is often less than 10^3 cm^{-3} [Schröder et al., 2000b]. Aircraft generated aerosol mass is small compared to what is emitted and produced at the Earth's surface or by strong volcanic eruptions [IPCC, 1999].

Contrails

Contrails are line clouds often visible behind aircraft. Contrails form when the mixture of exhaust gases and cold ambient air reaches saturation with respect to liquid saturation. Liquid droplets then form, mainly by condensation of H_2O on exhaust particles, which soon freeze to form ice particles. If the atmosphere is cold enough, a contrail will always form even for zero

particle emissions from the aircraft engines because of condensation nuclei entrained into the exhaust plume from the ambient air.

Contrails evaporate quickly when formed in dry ambient air. The fractional global coverage by these contrails is less than 0.001% and hence of no importance to the climate [Ponater et al., 1996]. In humid air (above ice saturation) contrails can persist for hours and grow horizontally and vertically. About 10-20% of all jet aircraft flights occur in air masses that are humid enough to cause persistent contrails [Gierens et al., 1999b; Mannstein et al., 1999]. Aircraft exhaust often triggers cirrus clouds in these regions [IPCC, 1999].

Some contrail clouds can be identified and discriminated from natural cirrus clouds in satellite images based on the linear appearance of these contrails. Satellite data in 1996 and 1997 reveal that linear persistent contrails cover about 0.5-0.7% of the sky at noon over Europe in the annual average [Mannstein et al., 1999; Meyer et al., 2000, 2001]. This represents a lower bound for the actual contrail cover. The fraction of cirrus clouds with non-linear shape that originated from old contrails or from aircraft induced particles is unknown. The satellite data indicate a night-time contrail cover, which is about one third of that during daytime. The mean global cover by linear contrails has been estimated to be 0.1% for 1992 [Sausen et al., 1998], but this value is quite uncertain (possibly 0.02-0.2% [IPCC, 1999], see below). Future improvements in the overall propulsion efficiency will reduce the amount of heat released into the exhaust gases, thereby increasing the threshold temperature of contrail formation and, hence, increasing the contrail cover [Gierens et al., 1999a; Schumann, 1996, 2000a]. However, more efficient engines emit less carbon dioxide. The trade-off between these effects depends on the relative sensitivity of climate to contrails and carbon dioxide changes and on the scenario of future aviation [Schumann, 2000b].

Contrails cause a positive mean RF at the top of the atmosphere, in particular during night and over warm and bright surfaces [Meerkötter et al., 1999]. The radiative effects of contrails depend mainly on their coverage and optical depth, both of which are still not well known.

Cirrus Clouds

Some correlation between soot and ice particle concentrations has been measured in cirrus clouds that could indicate an aviation impact on ice particle formation [Ström and Ohlsson, 1998b]. Long term observations of cloud frequencies at some meteorological stations and some satellite data indicate strong increases of the frequency or cover of cirrus clouds [Boucher, 1999; IPCC, 1999]. The increases are particularly large in some regions with high air traffic density. The global trends suggest a cirrus cover increase of up to 0.2% since the beginning of jet aviation, in addition to the 0.1% cover by line-shaped contrails [IPCC, 1999]. The change in cirrus cover could not be conclusively attributed to aircraft emissions or any other causes.

Climate Effects

The radiative RF resulting from aircraft engine emissions are summarised in Figure 7.1, as estimated for IPCC [1999]. The uncertainty associated with several of these contributions is large. The best estimate of the RF caused by aircraft in 1992 (without cirrus changes) was assessed to be 0.05 Wm^{-2} or about 3.5% of the total RF by all anthropogenic activities. The resultant overall RF by aircraft (without cirrus changes) is a factor of 2-4 larger than the forcing by aircraft CO_2 alone. Some of the RF contributions need to be revised in a future assessment (see below).

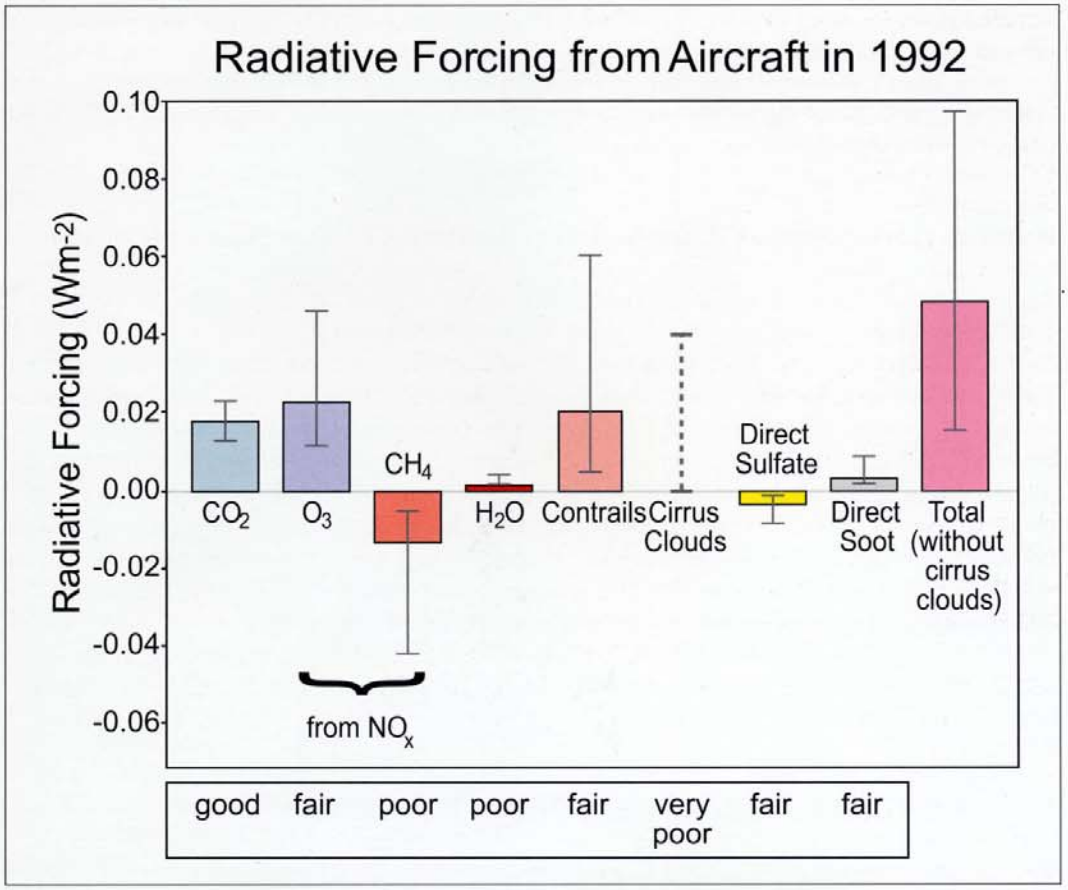

Figure 7.1 *Radiative forcing (Wm^{-2}) due to aircraft emissions in 1992 as estimated in IPCC [1999]. The columns indicate the best estimate of forcing. The error bars denote the range within which the best-estimate value is expected with a two-third probability. The available information on cirrus clouds is insufficient to determine either a best estimate or an uncertainty range; the dashed line indicates a range of possible best estimates. The estimate for total forcing does not include the effect of changes in cirrus cloudiness. The evaluations below the graph ("good", "fair", "poor", "very poor") are a relative appraisal associated with each component and indicates the level of scientific understanding. Reproduced by permission of Intergovernmental Panel on Climate Change, Geneva, and Cambridge University Press.*

For the range of scenarios considered in that assessment, the forcing is projected to grow to between 0.13 and 0.56 Wm^{-2} in 2050, i.e., 2.6-11.0 times the value in 1992. These estimates of forcing combine the effects from changes in concentrations of CO_2, O_3, CH_4, H_2O, line-shaped contrails, and aerosols, but do not include possible changes in cirrus clouds.

The emissions of NO_x cause changes in O_3 and CH_4, and their influences on the RF are of similar magnitude but have opposite sign. The latitudinal structure of the various forcings is different so that the net regional radiative effects do not cancel. Changes in tropospheric O_3 are mainly in the northern hemisphere, while those of CH_4 are global.

The state of scientific understanding of the RF of the various emissions has been evaluated in IPCC [1999] as indicated in Figure 7.1. The error bars and the scientific uncertainties are

largest for the complex impact of NO_x on CH_4 reduction, for contrails, and, in particular, for the indirect effects of aviation on cirrus cloud cover and changes in cirrus properties. New results on these aspects will be reported below. Up to now, a global climatic impact of aviation could not be detected in observations, and even regional effects will be difficult (if not impossible) to identify.

Radiative Forcing (RF) and Ultraviolet (UV) Radiation Effects of Supersonic Aviation

About 13 supersonic civil aircraft of type Concorde were in operation until the 25th July 2000. Their effect on the global atmosphere can be neglected compared to the effects of the far larger fleet of subsonic aircraft. Plans for a new fleet of supersonic aircraft have been discussed but no definite decision has been made to develop such a fleet [IPCC, 1999]. Supersonic aircraft would cruise at an altitude of about 16-24 km and contribute to changes in stratospheric O_3, other trace gases and aerosols. Supersonic aircraft consume more than twice the fuel per passenger-km compared to subsonic aircraft. The calculated RF of supersonic aircraft depends on the treatment of H_2O, O_3, and aerosols in models, which are difficult to simulate accurately. However, it is estimated that civil supersonic aircraft cause a five times larger forcing than for a fleet of subsonic aircraft providing the same transport capacity [IPCC, 1999]. The effect of introducing a fleet of 500 civil supersonic aircraft (Mach 2.4, emission index for NO_x of 5 g kg^{-1}) is to reduce the stratospheric O_3 column in the northern hemisphere by 0.4% (range -2.5 to +0.5%) [Kawa et al., 1999; Kinnison et al., 2001], and to increase the erythemal dose rate by a similar amount [IPCC, 1999].

7.3 PROGRESS IN UNDERSTANDING FROM RECENT STUDIES

This chapter summarises recent results concerning the open questions listed in the Introduction (Section 7.1) and related topics. The report concentrates on the results of the atmospheric research with respect to aviation impact in European programs and some related NASA projects, as listed in Table 7.1.

7.3.1 Composition of aircraft emissions and their role in aerosol particle formation

Plume Structure

An aircraft exhaust plume is characterised by its physical structure (geometry, dynamics) and chemical composition. In the jet engine compressed air is mixed with fuel in the combustion chamber and ignited. The hot gases expand through the turbine section of the engine while cooling from about 1600 K to 600 K before exiting the engine in what is termed the *jet regime* [e.g., Garnier and Laverdant, 1999], see Figure 7.2a. Behind the engine exit the hot exhaust cools quickly by mixing with ambient air and reaches ambient temperatures to within a few degrees after about one second. The double vortex generated by the flow over the wings captures most of the exhaust and descends below the flight level due to momentum conservation. This is termed the *vortex regime* [Gerz et al., 1998], see Figure 7.2b. Some of the exhaust may escape from the vortex system and form a veil of exhaust that remains at the flight level or even ascends [Sussmann, 1999]. The vortex system is inherently unstable and eventually breaks up into smaller scale turbulence [Gerz and Holzäpfel, 1999]. After 3-5 minutes, the aircraft induced turbulence has ceased and the ambient air motions control further spreading. This is termed the *dispersion regime*, see Figure 7.2c.

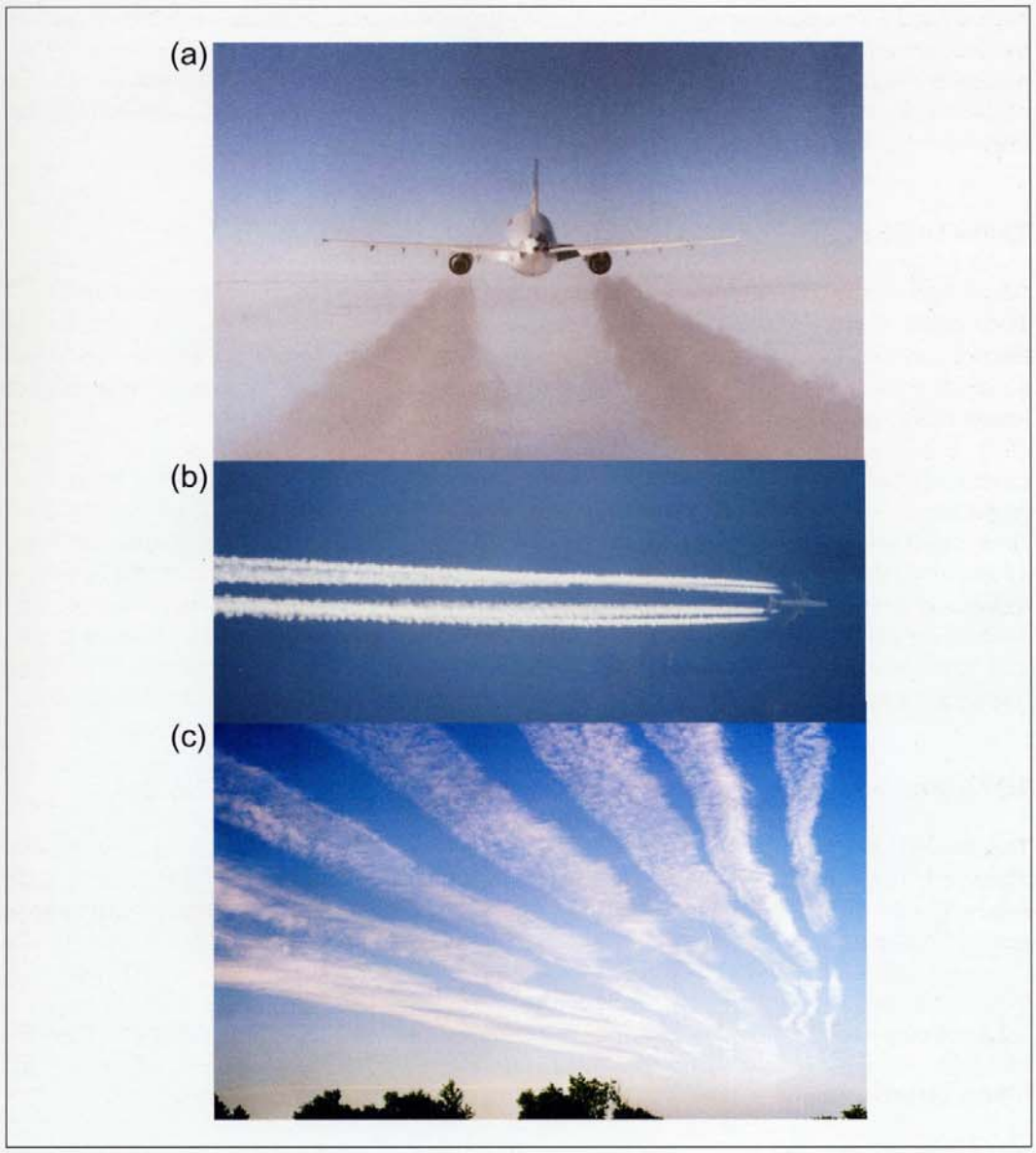

Figure 7.2 *Photos illustrating different regimes of aircraft plumes: (a) jet regime, (b) transition from jet to vortex regime, (c) dispersion regime. The photos show (a) contrails forming about 10 m behind the jet engines in the engine exhaust of an Airbus A310 as seen from the DLR-Falcon during SULFUR 4; (b) contrails forming from the four jet engine exhaust plumes before reaching the aircraft tail and then getting captured inside the two vortex tubes behind the aircraft cruising in the upper troposphere as seen from ground; (c) dispersing contrails forming from a sequence of aircraft flying along the same air route with some side-wind, as seen from ground in southern Sweden.*

Diffusion coefficients deduced from measurements and large-eddy simulations range from D_v=0-0.3 m^2s^{-1}, and D_h=5-20 m^2s^{-1} for the vertical and horizontal direction, respectively [Schumann et al., 1995; Dürbeck and Gerz, 1996; Gerz et al., 1998]. A logarithmic fit of the time dependent dilution factor ($N(t)=7000\ (t/t_0)^{0.8}$, t_0=1 s) based on observations of exhaust

tracers (e.g. CO_2 enhancements in the exhaust plume) measured in more than 80 cases behind various aircraft in the tropopause region and lower stratosphere has been found useful for estimating the concentration change with plume age. Due to dilution, individual plumes are very difficult to distinguish from the corridor background after a few hours [Schumann et al., 1998].

Plume Composition

An aircraft exhaust plume contains species emitted by the engines, species formed in the plume from emitted species and atmospheric species that become entrained into the plume. The majority of the emitted species (gases and soot particles) are produced by combustion of kerosene with ambient air in the combustion chamber of the engine. In addition some emitted species originate from oil and from the erosion of metal parts.

Combustion of kerosene produces mostly CO_2 and H_2O (see Table 7.2). Besides these gases numerous trace species are formed including NO, NO_2, SO_2, hydrocarbons (HCs), and soot-particles. Among the emitted gases and gaseous products formed in the very young plume are condensable gases (Table 7.3). These may undergo condensation in the young plume leading to volatile aerosol particles and volatile coating of soot. Such particles, if large enough, may themselves act as condensation nuclei or may interact with soot to form condensation nuclei, and hence have an important role in the formation of contrails and perhaps even cirrus clouds. Therefore, condensable gases present in a young exhaust plume are of considerable interest.

Hydrogen Gases

Besides H_2O (1230±20 g of H_2O per kg of fuel; see Table 7.2), minor emitted H gases include HCs, OH, HO_2 and H_2O_2. (The amount of H_2 emissions is unknown.) Most OH formed in the combustor is consumed by self-reactions or reactions with NO etc. before reaching the engine exit and leaving the exit with a hardly detectable OH concentration [Böckle et al., 1999]. The emission index of OH has been deduced from measured HONO, HNO_3, NO, and NO_2 concentrations in exhaust plumes using a chemical model including plume dilution for more than a dozen aircraft [Tremmel et al., 1998; Schumann et al., 2000a], see Table 7.3. The OH-radical is indirectly involved in aerosol formation by producing gaseous H_2SO_4 [Kärcher et al., 1996a; Gleitsmann and Zellner, 1998a], which is an efficient aerosol precursor.

Carbon Gases

The most abundant C-gas emitted is CO_2 (3160±60 g of CO_2 per kg of fuel; see Table 7.2). Minor C-gases include CO and HCs [Slemr et al., 1998, 2001], see Table 7.2. Of the C-gases some low volatility hydrocarbons are involved in aerosol formation, possibly including aldehydes, alkenes and alkynes [Yu et al., 1999]. Low volatility hydrocarbons have been identified, e.g., in car engine exhausts [Jacobson et al., 1999; Zervas et al., 1999], but the chemical composition of these condensable gases has not yet been identified with certainty. Oxygenated hydrocarbons were identified from chemiion measurements in exhaust plumes [Kiendler et al., 2000a, b]. The importance of condensable organic matter was deduced from the large volume of volatile aerosol found in aircraft plumes even when the aircraft burned fuel with very low sulphur content [Kärcher et al., 1998b; Yu et al., 1999; Schumann et al., 2001], see below.

Nitrogen Gases

The most abundant N-gases emitted are NO and NO_2 (see Table 7.2). The knowledge about the emission factors of NO_x from aircraft has been strongly increased in recent years by measurements in the plume of cruising aircraft. NO and NO_2 may be measured by chemiluminescence techniques and Fourier transform infrared spectroscopy methods [Schulte and Schlager, 1996; Haschberger and Lindermaier, 1997; Schäfer et al., 2000; Schulte et al., 1997]. A small fraction of the N-gases emitted includes HNO_2 and HNO_3 (Table 7.2). These are formed via reaction of OH with NO and NO_2 respectively. Both HNO_2 and HNO_3 have been measured by chemical ionisation mass spectrometry in aircraft exhaust plumes at cruise altitudes [Arnold et al., 1992; Tremmel et al., 1998]. The equivalent emission indices derived from these data are 0.08-0.8 g per kg HNO_2 and 0.02-0.3 g per kg HNO_3 (Table 7.2), as summarised in Schumann et al. [2000a]. Since both HNO_2 and HNO_3 are formed via OH, an effective OH-concentration could be inferred from the HNO_2 and HNO_3 data [Tremmel et al., 1998; Schumann et al., 2000a]. Among the N-gases, HNO_3 is a condensable gas at least under conditions of very low plume temperatures (<200 K) and when the humidity is low so that water-ice does not yet form [Arnold et al., 1992]. In addition some HNO_3 may be taken-up by H_2SO_4/H_2O aerosols [Kärcher, 1996] and by contrail particles at high relative humidity and at temperatures below 222 K [Gleitsmann and Zellner, 1999]. Measurements in cirrus clouds indicate that only a few percent of available HNO_3 is taken up by ice clouds [Schlager et al., 2000].

Sulphur Gases

The most abundant S-gas is SO_2 (Table 7.2). SO_2 measurements in aircraft exhaust plumes were found to be consistent with average fuel sulphur contents [Arnold et al., 1994; Schumann et al., 1998]. According to models, fuel sulphur is oxidised mainly to SO_2 in the combustor [Brown et al., 1996a]. In the turbine a small fraction of SO_2 experiences further oxidation by O-atoms leading to SO_3. Additional SO_2 oxidation via OH-radicals takes place downstream of the combustor exit but mostly still upstream of the engine exit plane [Brown et al., 1996a; Tremmel and Schumann, 1999]. Via reaction with water vapour, SO_3 becomes converted to gaseous H_2SO_4 mostly at plume ages smaller than 10 ms [Reiner and Arnold, 1993; 1994]. Gaseous H_2SO_4 has a very low vapour pressure and likely represents the most important aerosol precursor. Hence, the conversion fraction of fuel sulphur to H_2SO_4 is a very important parameter. Gaseous H_2SO_4 was detected in fuel combustion experiments in the laboratory and in jet engine exhaust at ground-level [Frenzel and Arnold, 1994]. From these measurements a fraction, ε, for fuel sulphur conversion to H_2SO_4 of ε>0.4% was inferred. More recent measurements yielded $\varepsilon \approx 1.2\%$ [Arnold et al., 1998b]. Early model studies of OH-induced H_2SO_4-formation yielded 0.5-2.0% [Kärcher et al., 1996a; Gleitsmann and Zellner, 1998]. Here the initial OH-mixing ratio was assumed as a free model parameter. The uptake of SO_2 in aqueous sulphuric acid solution is too small to be important compared to the gas phase oxidation by the reactions with OH [Rattigan et al., 2000]. A model of OH-induced H_2SO_4 formation by Tremmel et al. [1998] yielded $\varepsilon \approx 0.4$-0.6%. This model builds on OH concentrations inferred from the HNO_2- and HNO_3-measurements. For O- and OH-induced H_2SO_4 formation starting in the combustor of the engine, models predict ε values of 10% and more [Brown et al., 1996a; Lukachko et al., 1998]. A small fraction of the SO_3 is formed in the combustor but most is formed inside the engine between the combustor and engine exit [Starik et al., 2001]. The H_2SO_4 is formed mainly at the end and outside of the engine. The uncertainty

of the computed conversion rate is high because of missing data on the reaction rate and equilibrium constant of SO_2 with OH at temperatures >300 K [Tremmel and Schumann, 1999].

Direct measurements of H_2SO_4 in aircraft exhaust plumes at cruising altitudes became available recently using a novel aircraft-based chemical ionisation mass spectrometry instrument [Curtius and Arnold, 2001]. These measurements which were made first during recent SULFUR-campaigns yielded ε>0.34% [Curtius et al., 1998] and ε=3.3±1.8% [Curtius et al., 2001], see Figure 7.3. Upper bounds of ε of about 1.8-10% (depending on engine and the fuel sulphur content) can be derived from a combination of these direct measurements with aerosol measurements and models [Schumann et al., 2001]. Early, indirect estimates claimed far larger conversion fractions [Fahey et al., 1995; Miake-Lye et al., 1998]. However, recent studies reveal that the indirect means are not accurate enough to determine the conversion fraction, and that the measured amount of SO_2 is consistent with nearly all of the fuel sulphur appearing as gas phase SO_2 in the exhaust [Brock et al., 2000; Hunton et al., 2000; Schumann et al., 2001]. Model studies show that ε increases with temperature and pressure at combustor exit in the engine, and is, hence, engine dependent [Miake-Lye et al., 2000; Schumann et al., 2001; Starik et al., 2001].

For a typical fuel sulphur content of 400 μg per g, and ε=3.3%, the engines emit 0.04g H_2SO_4 per kg (Table 7.3). This value exceeds the soot emission index of 0.01 g per kg of modern jet engines. The emission index for organic condensable material is about 0.01-0.03 g per kg (Table 7.3). Therefore sulphuric acid remains to be the most important precursor of volatile aerosols formed in aircraft exhaust plumes unless the fuel sulphur content decreases below about 100 μg per g.

Chemiions (CIs)

One of the most important findings of recent years is the fact that aircraft engines emit gaseous ions, so called chemiions [Arnold et al., 1998b, 1998c, 2000a] which are important as aerosol-precursors [Frenzel and Arnold, 1994; Yu and Turco, 1997, 1999, 2000]. CIs are formed during combustion in the engine. CIs promote particle-formation in two ways: through electrostatic forces the net charge stabilises small molecular clusters and increases the flux of condensable gas molecules to the cluster. Primary CIs are formed in the combustor via radical-radical reactions and subsequently undergo a rapid chemical evolution via ion-molecule reactions involving plume gases which leads to large cluster ions.

The concentration of charged particles formed by combustion-induced CIs is high at engine exit, about 10^9 cm^{-3} [Arnold et al., 2000b]; i.e. of the order 10^{17} kg^{-1} of fuel burned, see Figure 7.4. The CI concentration decreases steeply with increasing plume age due to ion-ion recombination in the early jet and due to dilution, as discussed also by Sorokin and Mirabel [2001].

Ion mass spectrometric measurements in jet engine exhaust have revealed the chemical nature of CIs [Frenzel and Arnold, 1994; Arnold et al., 1998b; Kiendler et al., 2000a, b]. It was found that "light" negative CIs are mostly of the type $HSO_4^-(H_2SO_4)_m(H_2O)_n$ ($m \leq 2$, $n \leq 3$) and that some negative CIs also contain HCs. Positive CIs are mostly composed of HCs, in agreement with theoretical arguments [Yu et al., 1999]. Some of these HCs have been further identified as oxygenated HCs [Kiendler et al., 2000a]. The positive and negative CIs can be very massive (exceeding 8500 atomic mass units), even for nearly sulphur-free fuel (2 μg per g), see Figure 7.5

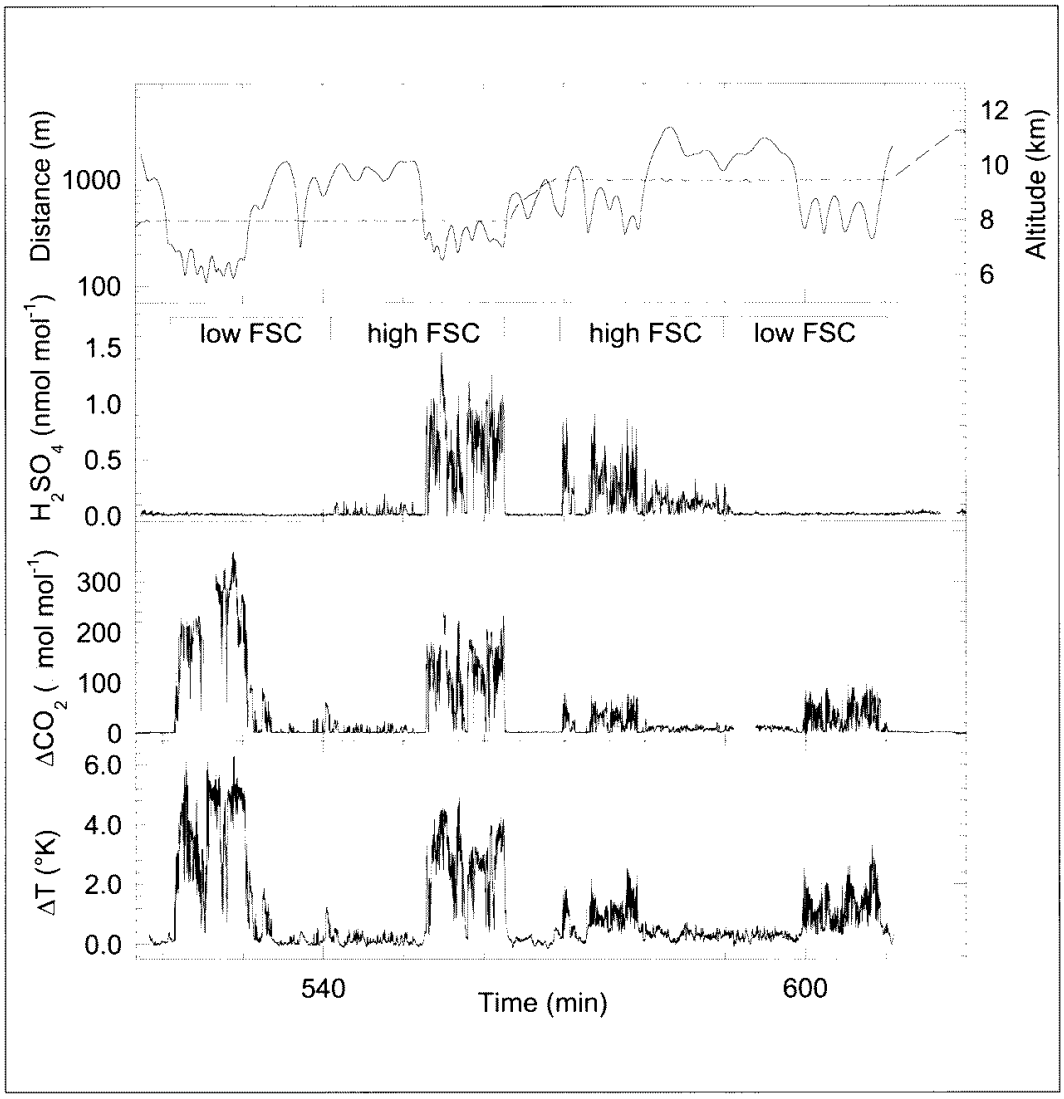

Figure 7.3 *First measurements of sulphuric acid concentration and the conversion efficiency ε of fuel sulphur into sulphuric acid in the engine exhaust gases of a cruising jet aircraft. During flights of the DLR-Falcon behind the DLR test-jet aircraft ATTAS, at 8.0-9.5 km altitude, clear increases in carbon dioxide ($\Delta CO_2 \approx 200$ μmol/mol) and temperature ($\Delta T \approx 3.3$ K) were measured when entering the exhaust plume at short distance (down to 70 m). The CO_2 and temperature increases are consistent when normalised with the emission index of CO_2 times the ratio of molar masses of air and CO_2 (3.15×29/44), and the ratio of effective fuel combustion heat released to the exhaust and the specific heat capacity of the exhaust gas [(1-η) Q/c_p=35,000 K], respectively. When burning fuels with high fuel sulphur content (FSC=2700±300 μg/g) on the ATTAS, the measurements show clearly correlated increases in sulphuric acid ($\Delta H_2SO_4 \approx 1$ nmol/mol; measured by MPIK Heidelberg). The ratio of signals implies $\varepsilon = (\Delta H_2SO4/\Delta CO_2)(32/44)\ EI_{CO2}/FSC) \approx 0.4\%$ (where 32/44 is the ratio of molar masses of S and CO_2). Because of potential wall losses within the instrument and the inlet, this value represents a lower bound to the actual conversion fraction [Curtius et al., 1998]. As can be also seen from this figure, no increase in ΔH_2SO4 was detectable when the ATTAS engines were burning fuel with low FSC (22±5 μg/g). In order to exceed background fluctuations and statistical scatter, the conversion fraction at low FSC has to be larger than 2.5 times the value at high FSC. More recent measurements behind another aircraft (a B-737) suggest a conversion fraction of 3.3±1.8% [Curtius et al., 2001].*

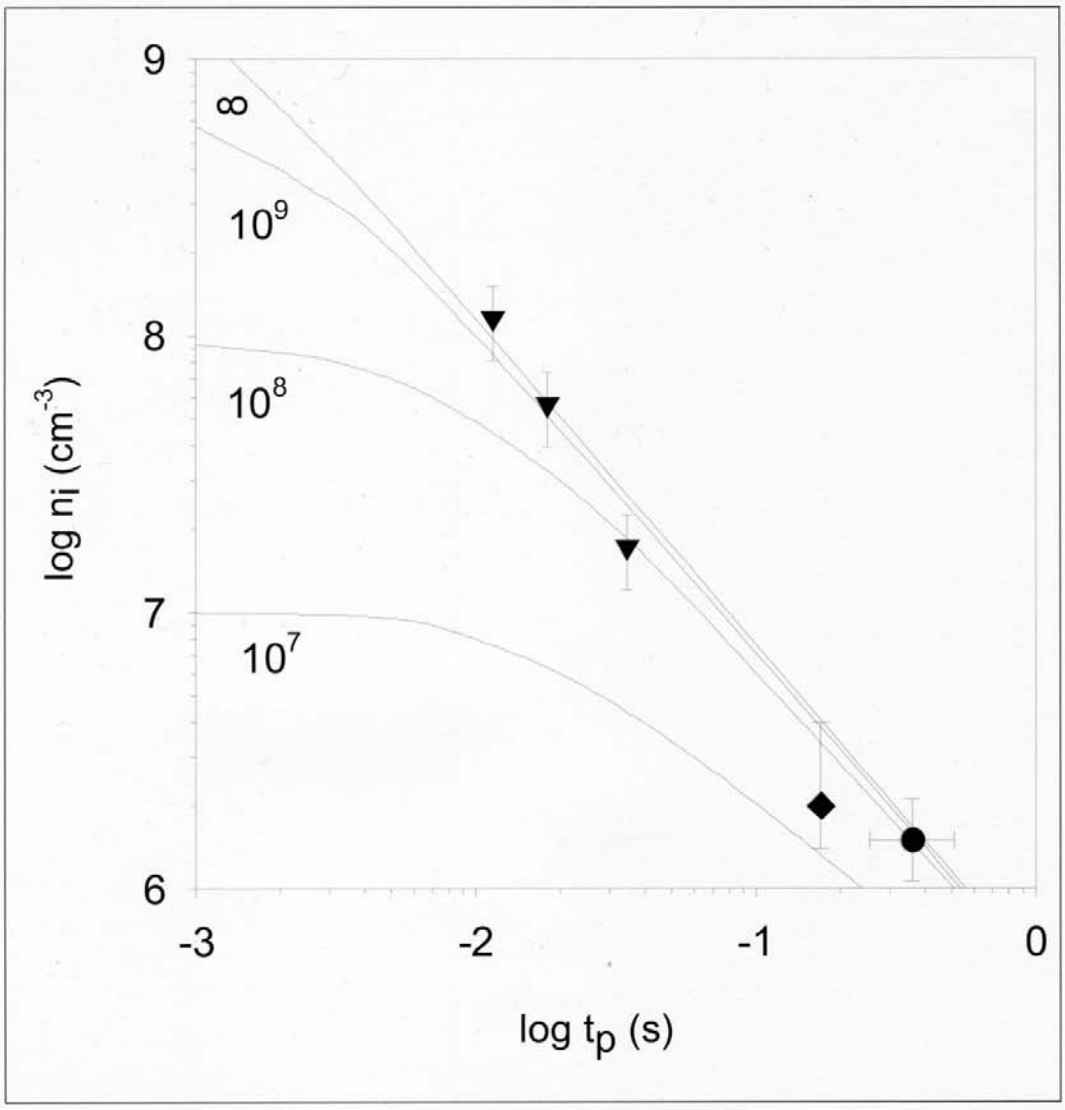

Figure 7.4 *Total concentration of positive chemiions n_i measured in the exhaust of a jet engine (ATTAS, Rolls Royce/SNECMA M45HMk501) at ground level as a function of plume age t_p. The curves show model results considering ion depletion by ion-ion recombination and plume dilution for 4 initial ion concentrations (10^7 cm^{-3} and larger) at the engine exit. The symbols with error bars refer to various measurement cases. [Arnold et al., 2000b].*

[Wohlfrom et al., 2000a, 2000b]. The fractional abundances of CIs with mass numbers >8500 atomic mass units (in the range 0.2-0.7) were found to increase with fuel sulphur content and to be larger for negative CIs than for positive ones. Probably the growth of these CIs involves organic trace gases. If composed mostly of an H_2SO_4/H_2O mixture, a CI with a mass number of 8500 would have a diameter of about 3 nm, which is comparable to the size-detection limit of present condensation nucleus counters. Hence most of the smallest particles detected by such counters may actually have originated from CIs and their electrically neutral recombination products [Arnold et al, 2000b].

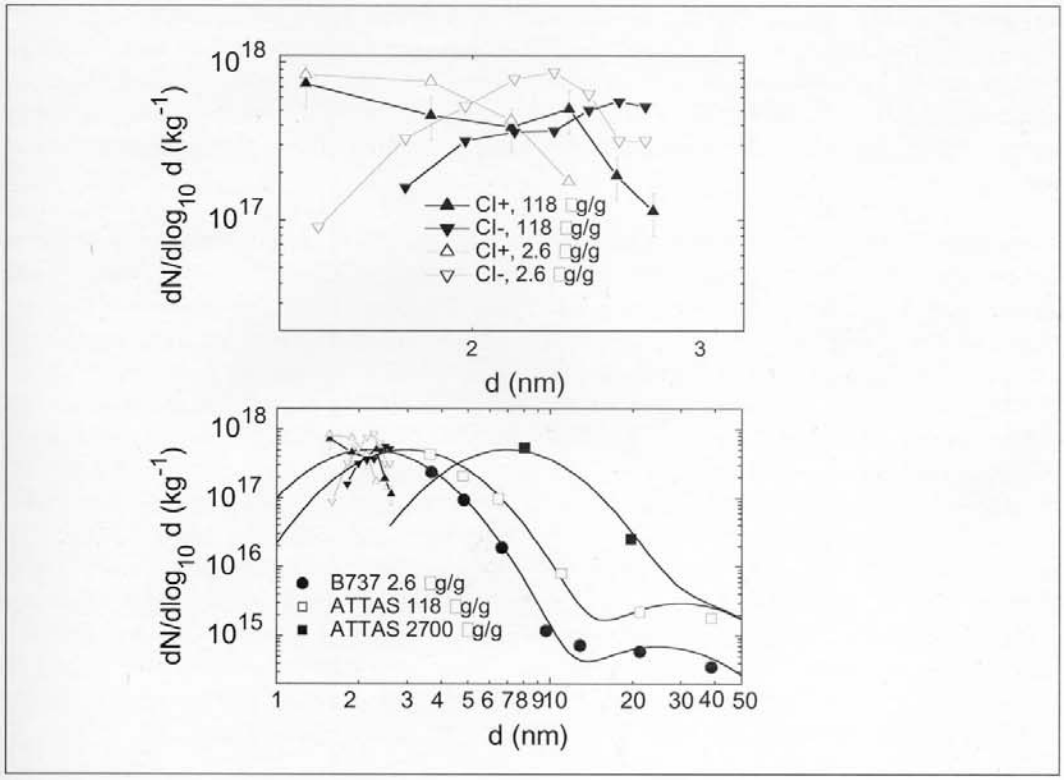

Figure 7.5 *Number N of particles per unit mass of fuel burned and per logarithmic interval of particle diameter versus particle diameter d, showing size distributions of chemiions (top and bottom panel) measured by Wohlfrom et al. [2000] with the Large Ion-Mass Spectrometer (LIOMAS) in the exhaust plume behind the ATTAS and plume aerosol particles (bottom panel) measured by Schröder et al. [2000b] with condensation particle counters (CPCs) for different fuel sulphur contents (FSCs). The three bimodal distributions (bottom panel) represent parameterisations of measurements behind the B737 (2.6 μg/g FSC), and the ATTAS (118 μg/g and 2700 μg/g FSC). The CI data are for 2.6 and 118 μg/g FSC (open and full symbols) for positive (CI+, triangle upward) and negative ions (CI-, triangle downward). LIOMAS data have been normalised to fit the aerosol data assuming a total number of particles (chemiions of either sign, and condensation nuclei) corresponding to a particle emission index of 2.0 and $2.4 \cdot 10^{17}$ kg^{-1} for 2.6 and 118 μg/g FSC, respectively. [Schumann et al., 2001].*

Soot Aerosol Particles

During combustion small non-volatile carbon soot particles are formed, which are nearly spherical with typical diameters of 30-60 nm [Bockhorn, 1994]. Soot emissions from aircraft engines are specified by the International Civil Aviation Organisation in terms of smoke number measurements, which is a filter stain reference method. A correlation between smoke number and soot mass concentration was used to estimate the mean mass emission index of black carbon by the globally operating aircraft fleet to be 0.04 g per kg [Petzold et al., 1999a]. Older engines have higher emission indices, whereas more modern engines such as CFM56-3B1 on a B737 emit much less, 0.01 g soot per kg fuel. On the order of 10^{14}-10^{15} kg^{-1} soot particles are emitted depending on engine type and power setting [Petzold and Döpelheuer, 1998].

The composition of soot is difficult to determine. Quantitative single particle analysis methods that cover the whole pertinent aerosol size distribution, ranging from a few nanometres to several hundred nanometres, are still to be developed [Murphy et al., 1998]. Soot has to be collected on filters or similar devices to obtain sufficient mass for analysis. The soot may change when captured on the filter and then exposed for some time to the ongoing stream of exhaust gases.

Aeroengine combustor soot differs from pure graphitic soot. Soot particles collected on filters are mainly composed of carbon, but also contain sulphate (0.4-5.4%), with only a slight dependence on engine power setting [Petzold and Schröder, 1998]. An elemental analysis shows large (order 10%) mass fractions of O, S, and N, in soot exposed for some time to the exhaust stream [Zellner, 2000]. At the exit of several specific combustors, soot concentrations of 10^6-10^7 cm^{-3} have been measured during the CHEMICON project [Harrison et al., in Zellner, 2000], with modal diameters ranging from 40-70 nm. The specific surface area of the microporous soot was measured to be 75 m^2 per g for a combustor soot and 64 m^2 per g for a laboratory prepared kerosene soot. Different from graphitic black carbon, combustor soot particles appear to be hydrophilic before reaching water saturation and may therefore serve as nuclei for water condensation without prior activation [Chughtai et al., 1999; Popovitcheva et al., 2000, 2001]. In the exhaust plume, the soot particles quickly build complex aggregates causing a second mode of larger particles between 100 and 500 nm [Sheridan et al., 1994]. Their size, however, is difficult to characterise due to the fractal or fluffy shape acquired during aggregation. The change of aviation soot properties in the atmosphere with increasing age (after a few minutes) has not yet been determined.

Volatile Aerosol Particles

Previous measurements [e.g., Schröder et al., 1998] provided much progress in identifying the number of ultrafine particles, but the size spectrum of particles was still poorly defined because of missing continuity from the smallest clusters to the particles which can be measured optically at sizes of ~100 nm and larger. Therefore, particle size spectra of aerosols particles with diameters from 3 to 60 nm were measured in young exhaust plumes, very close to the emitting aircraft (>30 m) at cruise during the sixth SULFUR experiment with an innovative cascade of nine particle counters operating in parallel with different lower size detection limits. By normalisation with the simultaneously measured CO_2 concentration, the apparent emission indices were determined [Brock et al., 2000; Schröder et al., 2000a].

Volatile aerosol particle concentrations in the aircraft plumes strongly increase as diameter decreases from 60 nm toward the sizes of large molecular clusters (diameter ≈3 nm), illustrating that apparent particle emissions are extremely sensitive to the smallest particle size detectable by the instrument used, see Figure 7.6. Contrail formation and plume age alone can influence the number of detected ultrafine volatile particles within an order of magnitude, as well. The observed particle emissions decreases non-linearly with fuel sulphur content and become independent of fuel sulphur below 100 μg per g.

There are experimental indications that non-sulphate compounds – probably low-volatility hydrocarbons [Kiendler et al., 2000b; Wohlfrom et al., 2000] – dominate the volatile aerosol composition as the fuel sulphur content decreases below about 100 μg per g. For low fuel sulphur content, a sulphur conversion efficiency of even 50% is not enough to explain the large volume of volatile material measured with particle counters [Schröder et al., 1998, 2000b;

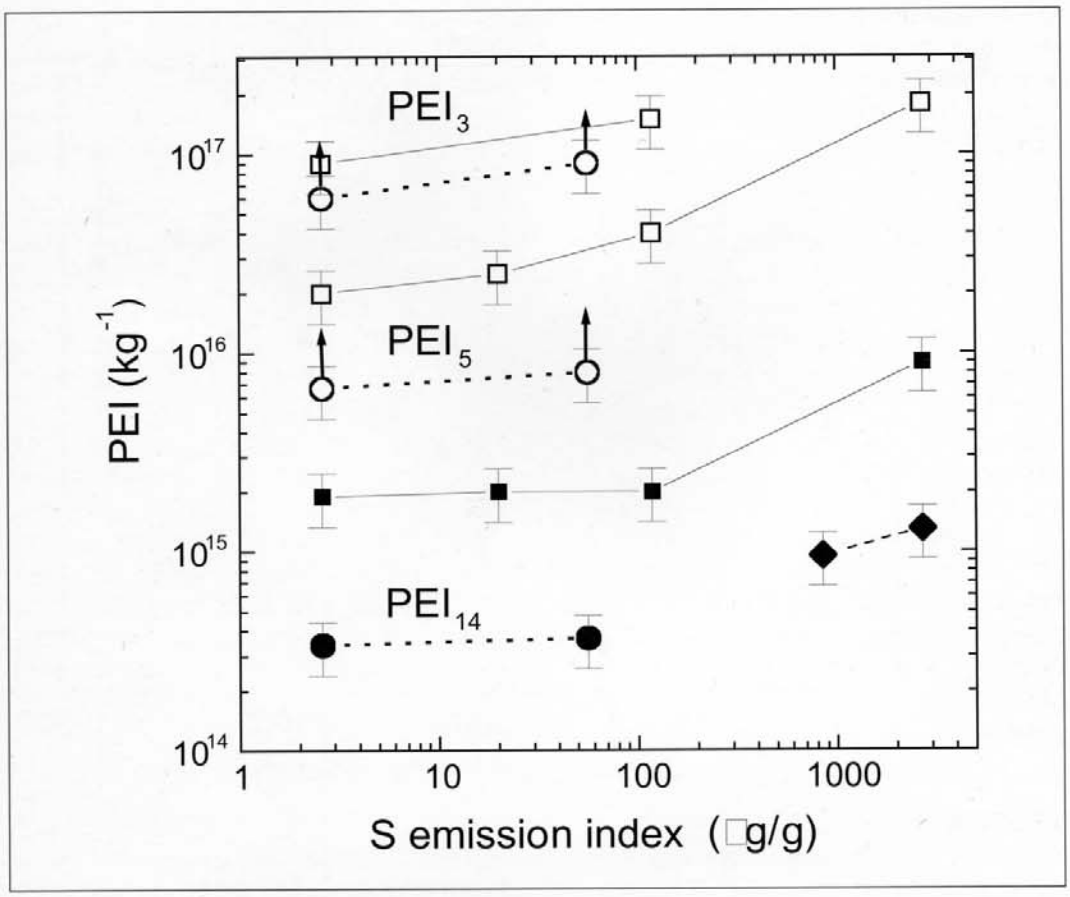

Figure 7.6 *Emission index of detectable volatile particles (PEI_d, the index d refers to the lower detection limit of particle diameters; d=3, 5, and 14 nm), measured in aircraft exhaust plumes that do not cause a contrail, versus sulphur emission index, behind the ATTAS aircraft with RR M45H Mk501 engines (squares), Boeing 737-300 aircraft with CFM56-3B1 engines (circles), and Airbus 310-300 with CF6-80C2A2 engines (diamonds). [Brock et al., 2000; Schröder et al., 2000a].*

Kärcher et al., 1998a], and it has been suggested therefore that part of the volatile material results from condensable exhaust HCs. Further arguments to support this conclusion are given by Yu et al. [1999].

Kärcher et al. [2000] provided a model to explain the wide variance of apparent particle emission indices in exhaust plumes (not forming contrails) observed during SULFUR 5 and 6 [Schröder et al., 1998, 2000a], behind a Concorde [Fahey et al., 1995], a F-16 aircraft [Anderson et al., 1999a] and behind a wide-body aircraft during POLINAT [Schumann et al., 2000a]. The model shows that this index depends on the lower cut-off size of the particle counters, the plume age, the fuel sulphur content, the conversion efficiency ε and the number of CIs available from the engine. The model assumes that the number of CIs available determines the number of volatile particles formed. The amount of sulphuric acid (depending on fuel sulphur content and the conversion efficiency ε) and the amount of condensable organic matter together control the size of the particles formed. Coagulation and dilution control the time scales of particle growth. Using this model, the measured apparent emission indices can be

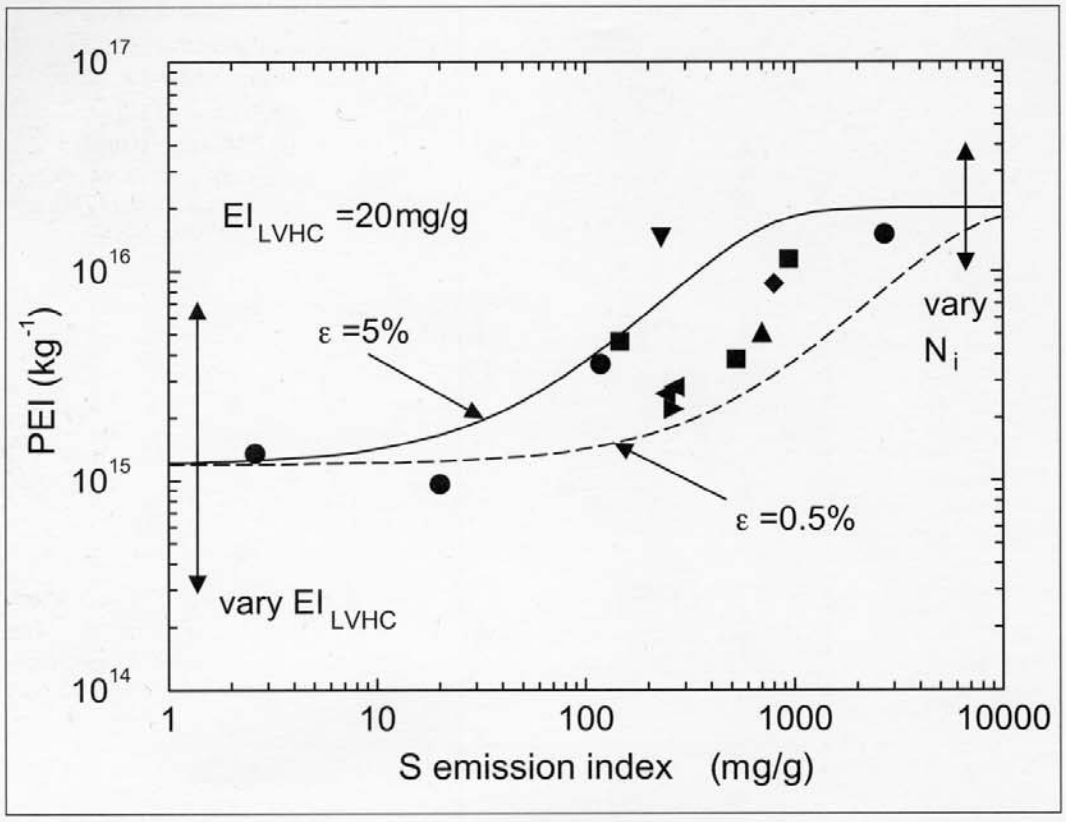

Figure 7.7 *Emission index of detectable volatile particles versus sulphur emission index from various measurements, normalised to plume age 3s, particles diameters >5 nm, 20 μg/g of low-volatility hydrocarbons, and various values of conversion fraction ε of fuel sulphur to sulphuric acid. The arrows indicate the changes in particle emissions for the expected range of variations in the emission indices of low volatility hydrocarbons (EI_{LVHC}) and chemiions N_i per unit mass of burned fuel leaving the engine. [Kärcher et al., 2000].*

normalised to a given plume age (3 s), emission index of low volatility hydrocarbons (20 μg per g), and cut-off size of the particle counters (5 nm), see Figure 7.7. As a consequence, the data are consistent with volatile particle emissions of $1.5\text{-}4\times10^{17}$ kg^{-1}, independent of environmental conditions, engine type, and for fuel sulphur contents ranging between 2.6 and 2700 μg per g.

7.3.2 Influence of contrails and aerosols on cirrus clouds and chemical processes

For recent reviews of the present knowledge and uncertainties see Kärcher [2000], Lee et al. [2000], and the proceedings of the European Workshop "Aviation, Aerosols, Contrails and Cirrus Clouds" (A^2C^3) [Schumann and Amanatidis, 2000].

Contrail Formation

The white trail of ice formed in the wake of an aircraft at high altitude is the most obvious atmospheric effect caused by aircraft emissions. These line-shaped clouds or contrails are

formed when the mixture of hot and humid exhaust gases from the engines and cold ambient air becomes saturated with respect to liquid water. The threshold temperature for onset of contrails can be predicted to better than 1 K by the so-called Schmidt-Appleman criterion, which depends on the emission index of water, ambient pressure, ambient relative humidity (RH), combustion heat and overall propulsion efficiency (η) [Schmidt, 1941; Appleman, 1953; Schumann, 1996, 2000a]. Sometimes, aircraft cause cloud free stripes (distrails) in clouds [Duda and Minnis, 2001]. Given the right conditions, a contrail can form even without exhaust through disturbance of the vertical wind field by the aircraft [Gierens and Ström, 1998].

The stratosphere is generally too warm and dry for contrails to form. However, if the temperature is low enough a short contrail can form even in the hypothetical case of air containing no ambient water vapour at all. A contrail behind a Concorde aircraft cruising supersonically in the rather cold polar vortex during the French ZEBRE experiment at 16 km altitude was observed by a lidar from the Falcon aircraft flying below the Concorde on the 20th January 1995. The contrail formed because of low ambient temperature (–71°C) in spite of the dry stratosphere (5% RH). However the contrail was visible only for about 20-30 s [Gierens, 1996a].

With future improvement in engine technology, the propulsion efficiency (η) will increase, which will result in less energy being wasted as kinetic or internal energy with the exhaust. The effect of increased propulsion efficiency is to form contrails at a warmer ambient temperature. A change in η from today of about 0.35 to possibly 0.5 in the future lets contrails form already at about 500 m lower altitude or 3 K higher ambient temperature [Schumann, 2000a]. The effect has been verified experimentally, see Figure 7.8 [Schumann et al., 2000b].

The fact that contrails do not form when the plume reaches ice saturation, implies that fresh soot particles do not act as efficient ice nuclei [Busen and Schumann, 1995; Kärcher et al., 1998b; Schumann, 2000a; DeMott et al., 1999]. Instead, ice particles in contrails form only when reaching water saturation in the plume. Then small water droplets form (from

Figure 7.8 *Photo of an Airbus A340 with contrails (left) and a Boeing B707 without contrails (right) at 10.5 km altitude taken from the Falcon cockpit. [Schumann, 2000a].*

condensation nuclei which are available in large amounts from the exhaust aerosol) and quickly grow by water uptake, freeze, and grow as ice crystals. Although soot particles from aircraft engines may not be as hydrophobic as previously thought, they may not necessarily serve as ice nuclei. At least part of the soot particles are hydrophobic and they do not act as a cloud forming nuclei unless the supersaturation exceeds several percent [Kärcher et al., 1996b]. However, filter analyses obtained by Petzold and Schröder [1998] and the CHEMICON project, indicate that sulphur from the fuel enters the particles early, possibly even during the combustion process, which may make the particles more hydrophilic. Measurements show that soot hydrates more effectively with increasing fuel sulphur content. This is consistent with different colours of contrails with high and low fuel sulphur content under special illumination [Gierens and Schumann, 1996]. Model studies [Andronache and Chameides, 1997, 1998; Brown et al., 1996b; Gleitsmann and Zellner, 1998a, 1998b, 1999; Kärcher, 1996, 1998a, 1998b, 1999; Kärcher and Fahey, 1997; Kärcher et al., 1995, 1996a, 1996b, 1998a, 1998b; Zhao and Turco, 1995] also show that heterogeneous nucleation and plume evolution may convert soot particles into partially acid coated aerosols.

Pure water freezes homogeneously at a rate which decreases strongly with temperature and increases linearly with the volume of liquid water. The freezing rate becomes very large at temperatures below about –40°C [Pruppacher, 1995]. In the exhaust the volatile particles freeze homogeneously when the water fraction is large enough to overcome freezing suppression by acidic components. Koop et al. [2000] recently presented a new formulation for the formation rate of ice germs as a function of water activity, temperature and pressure. Water activity of a solution is the ratio of the vapour pressure over the solution to the vapour pressure of pure water [Pruppacher and Klett, 1997; pp. 110]. They show that homogeneous ice nucleation occurs (in less than a minute from germs with radius >0.2 μm) if the RH over ice exceeds 238.7-(0.398×T) for 175 K<T<233.5 K. The heterogeneous freezing process of liquid coated soot or metal particles is largely unknown but may be more important than homogeneous freezing unless the temperature is below the limit of homogeneous nucleation (below –40°C) [DeMott et al., 1999; Khvorostyanov and Curry, 2000]. For 1% supersaturation with respect to liquid water in the plume, most aerosols larger than a few nanometres serve as cloud condensation nuclei [Pruppacher and Klett, 1997]. Hence, the contrail properties depend little on the aerosol properties. However, the number of particles which get large and diluted enough by uptake of water to freeze does depend strongly on the degree of supersaturation (besides particle properties) and hence on the temperature difference with respect to the threshold temperature [Kärcher et al., 1998a].

Contrail Particles

Observations indicate that the primary particles on which contrail ice forms are most likely soot particles [Schumann et al., 1996, 2001; Petzold et al., 1997, 1998, 1999a, b; Kuhn et al., 1998]. In one experiment, about one third of the soot particles measured were involved in ice nucleation in contrails [Schröder et al., 1998]. Twohy and Gandrud [1998] and Petzold et al. [1998] identified also particles other than soot that may act as ice nuclei in the plumes. Ström and Ohlsson [1998b] measured a vertical gradient in the amount of absorbing material contained in contrail ice from individual plumes. This suggests that the relative importance of soot as ice nuclei may depend on where ice nucleation takes place in the plume and on the role of entrained ambient aerosols.

The question on how much aerosols impact cirrus clouds is the topic of the recent INCA experiments [Ström et al., 2000]. New *in situ* and remote sensing data on aerosols and cirrus

properties are now becoming available based on measurements. For the first time, differences in aerosols and cirrus properties in the southern and northern hemisphere have been determined within the INCA project. A clear inter-hemispheric contrast was found in terms of CO, O_3, NO, and NO_y. A large contrast in the concentration of small particles of various sizes and volatility properties between the northern and southern hemispheres has been observed which may be caused to some degree by aircraft emissions. The measurements in the clean atmosphere revealed often large ice particles of bullet rosette shape, and high RH above ice saturation.

As described in Section 7.3.1, the exhaust also generates many small volatile particles that could act as sites for condensation of water and subsequent freezing. Results from the series of SULFUR experiments show that the fuel sulphur content only marginally changes the conditions for contrail formation [Schumann et al., 1996; Petzold et al., 1997]. This is probably also true for any other impurity in the fuel. One reason for this is that even with a particle free exhaust the ambient air contains ample number of particles acting as condensation nuclei at the high humidity in the plume [Jensen et al., 1998a; Kärcher et al., 1998b].

The evolution of volatile particles in contrails (wet and cold plumes) differs from that in dry and warm plumes without contrails [Kärcher, 1999]. The residual particles from evaporating contrails may be more efficient ice nuclei for cirrus formation than fresh, more hydrophobic soot [DeMott et al., 1999]. However, it is very difficult to find and measure exhaust plumes when the contrail has evaporated and the trace (in terms of visible aerosols, measurable tracers or turbulence) of the aircraft is lost. Therefore, very little is known about the fate of aviation aerosols after leaving the young aerosols plume or contrail.

When contrails first become visible, a few ten metres behind the engine, they contain at least 10^4-10^5 cm^{-3} ice particles [Kärcher et al., 1996b]. After about a minute, the contrail is further diluted and composed of 10^3 cm^{-3} of small quasi-spherical crystals [Strauss et al., 1997; Gayet et al., 1998; Poellot et al., 1999]. During dilution, the integral number of ice particles within the contrail cross-section per unit flight path (typically 10^{11}-10^{12} m^{-1}) can grow slightly with plume age from freezing of entrained ambient haze droplets [Gierens and Ström, 1998]. As ambient air is entrained into the contrail, feeding more water vapour, the crystals grow and become more complex [Freudenthaler et al, 1996; Gayet et al., 1998]. Eventually, the crystal size distribution in contrails develops a shape very similar to natural cirrus clouds [Gayet et al., 1996; Ström et al., 1997; Schröder et al, 2000b]. The time it takes to transform a contrail to a cirrus-like cloud depends on temperature and humidity.

Contrails and Vortex Interaction

The vortex dynamics generated in the wake of an aircraft [Holzäpfel et al., 2001] is very important for the initial development of contrails. Freudenthaler [2000], Sussmann [1999], Sussmann and Gierens [1999, 2001], and Lewellen and Lewellen [2001] have studied details in contrail development caused by differences in the number and position of engines and different aircraft sizes. Under sub-saturated conditions, contrails of 2-engined aircraft evaporate mainly during the jet phase (<20 s) whereas, contrails of 4-engined aircraft often survive until the end of the vortex phase (ca. 2 min) [Sussmann and Gierens; 2001]. For supersaturated conditions, the persistent contrails resulting from a large and a small airliner have been found in numerical simulations to be similar [Lewellen and Lewellen, 2001].

Persistent Contrails

If ambient humidity is above ice saturation, the contrails may persist for many hours and travel great distances from where they were originally formed [Schumann, 1994; Minnis et al., 1998]. Contrail persistence is linked to the synoptic conditions that support high humidity and low temperatures, such as rising motions [Kästner et al., 1999; DeGrand et al., 2000]. Ice supersaturation occurs frequently (Figure 7.9). Gierens et al. [1999b] found that aircraft spend 13.5% of their flight time in regions saturated with respect to ice, where the mean ice-supersaturation was 15%. Occasionally, ice supersaturated regions were also found in the lowermost stratosphere just above the tropopause (defined in terms of O_3 threshold). The horizontal size of those high humidity regions varies strongly, but with a median value near 150 km [Gierens and Spichtinger, 2000]. Their vertical size is unknown. For long-lived contrails, wind-shear and turbulence are the most important mechanisms for the development and spreading of a contrail [Freudenthaler et al., 1995; Gerz et al., 1998; Freudenthaler, 2000]. The contrail may spread and become several kilometres wide in less than an hour [Jensen et al., 1998b; Gierens and Jensen, 1998; Gierens, 1996b, 1998]. Contrails also form within cirrus clouds [Sassen, 1997]. Such embedded contrails were assessed to have little effect on the cirrus [Schröder et al., 2000b], but may increase the cirrus emissivity [Poellot et al., 1999].

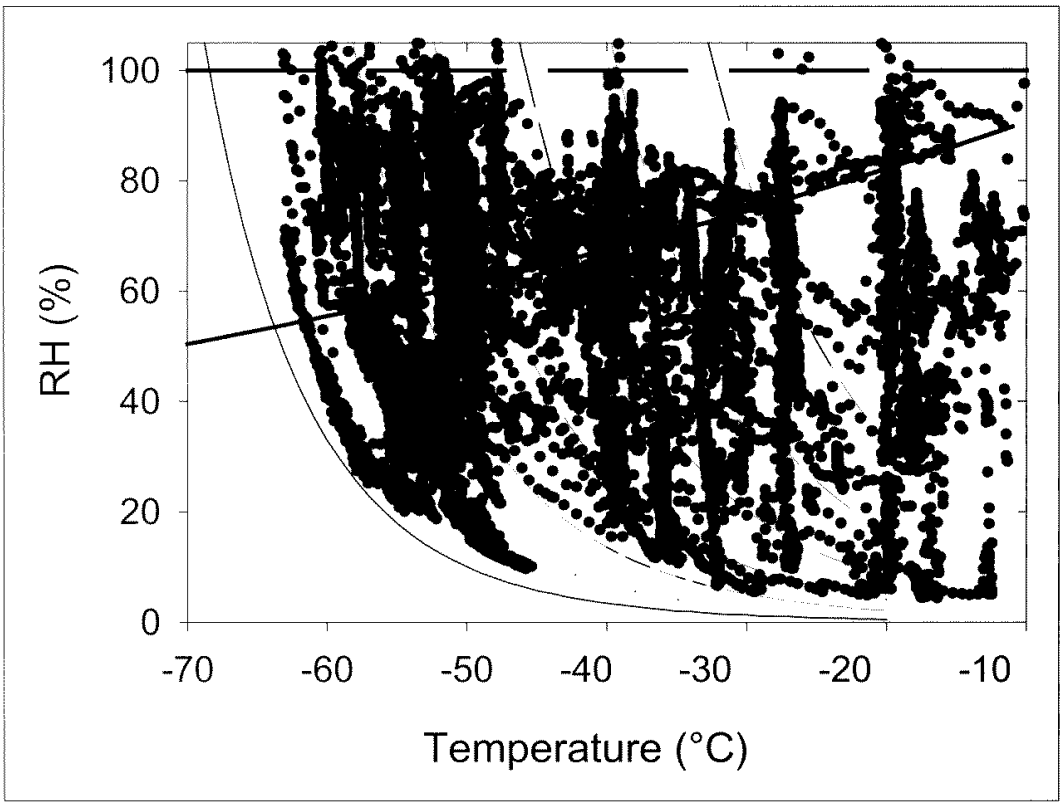

Figure 7.9 *Relative humidity with respect to liquid water versus ambient temperature. The thick horizontal dashed line denotes liquid saturation, the thick full curve denotes the relative humidity (RH) for ice saturation, and the thin curves with various line codings are lines of constant water mixing ratio. The symbols denote the measured data as derived from the LMD frostpoint hygrometer and the DLR temperature sensors during POLINAT 2. [Extended from Schumann et al., 2000a].*

Persistent contrails are composed of ice particles with a typical number density of 10-1000 cm^{-3}, see Figure 7.10. The ice water content in contrails (as in young cirrus) is temperature dependent [Meerkötter et al., 1999; Schröder et al., 2000b; Schumann, 2001] with values between 0.7 and 18 $\mu g\ m^{-3}$. At temperatures below about -50°C, ice particles in young persistent contrails have typically 5-50 μm diameter and hence are smaller than in ice clouds of natural origin [Betancor-Gothe et al., 1999; Poellot et al., 1999; Schröder et al., 2000b]. Measurements of strong depolarisation of lidar signals indicate that the ice particles are non-spherical [Freudenthaler et al., 1996; Sassen, 1997]. *In situ* observations with impactors of ice particle shapes, in some cases indicate close to spherical particles at least for low ambient temperatures [Strauss et al., 1997; Schröder et al., 2000b]. Other observations, e.g. with optical probes for larger particles, indicate particle shapes that deviate strongly from spherical [Jensen et al., 1998c; Liou et al., 1998]. Analysis of lidar data suggests that persistent contrails reach maximum optical depth (in the solar range near 550 nm wavelength) values between 0.05 and 0.5 [Sassen, 1997; Jäger et al., 1998]. Satellite data analyses reveal a mean optical depth near 0.1 over Europe [Meyer, 2000; Meyer et al., 2000, 2001]. Satellite data analysed by Minnis et al. [2000] suggest somewhat larger optical depth values over the USA. Much larger ice particles and larger optical thickness values may be found for contrails forming at high ice

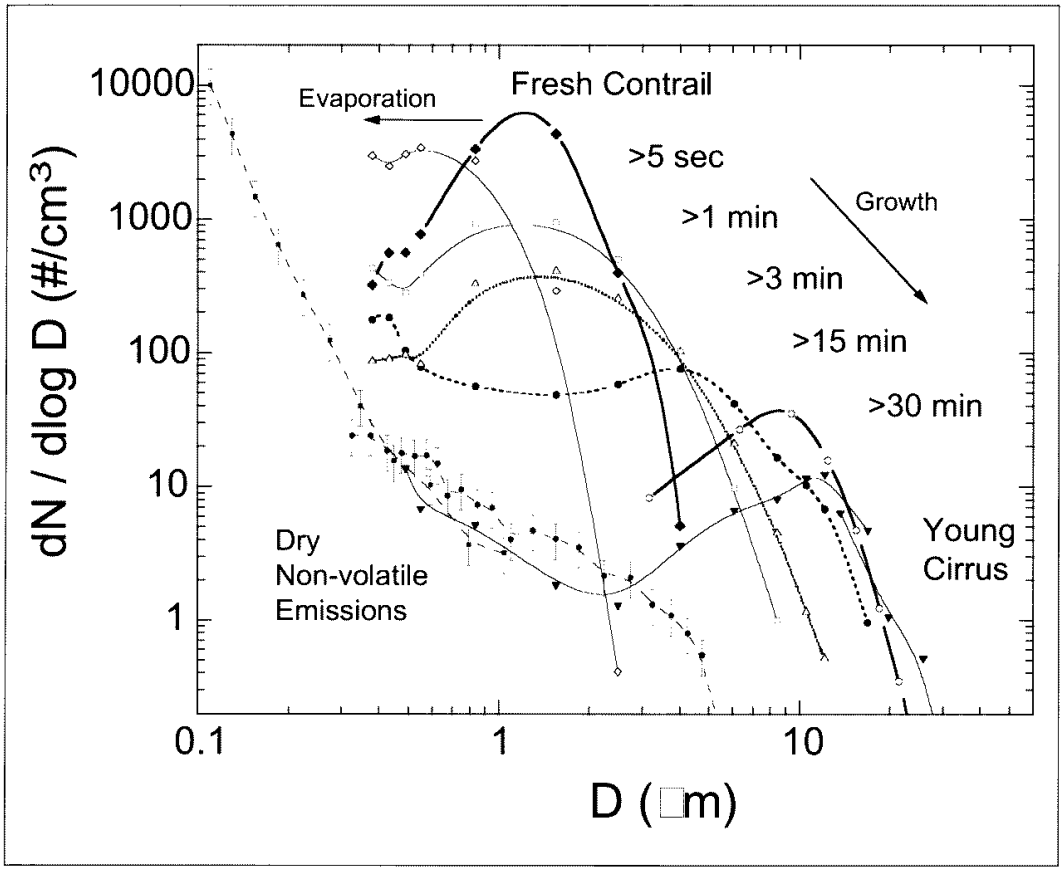

Figure 7.10 *Ice particle size spectra (number N of particles per volume and per logarithmic interval of particle diameter versus particle diameter D) measured with optical particle spectrometers in contrails of different ages and in young cirrus clouds and dry aerosol size spectrum (FSSP-300 spectrometer data and aerosol spectrometer PCASP probe). [Adapted from Schröder et al., 2000b].*

supersaturation, in particular at high temperatures (below the threshold temperature) when the amount of condensable water in the ambient air is high [Gierens, 1996b; Jensen et al., 1998b].

Contrail Cover

Contrail clouds can be identified and discriminated from natural cirrus clouds in satellite images based on their linear appearance. Depending on the sensors used, the contrail becomes detectable when reaching a sufficient width and optical contrast, typically after 10 minutes in NOAA-AVHRR data. Fresh contrails could also be identified from their smaller particle sizes compared to natural cirrus, but this parameter is more difficult to measure from space and still has to be exploited by more refined algorithms [Betancor-Gothe et al., 1999].

The fractional cloud cover of persistent contrails was estimated first by Bakan et al. [1994] by manually investigating satellite images from an Eastern North Atlantic and Western European region (30°W-30°E, 35-75°N). They found an average cloud cover from contrails in this region of around 1%. These values were deduced from satellite picture print-outs by visual inspection. Later analysis for Central Europe (where traffic density is higher) partly overlapping with the region considered by Bakan et al. [1994] gave smaller cover values [Mannstein et al., 1999; Meyer et al., 2001]. Mannstein et al. [1999] developed a fully automated method. Much care is needed to avoid false identification of contrails or underestimation of contrail cover over surfaces with strongly inhomogeneous surface temperatures [Meyer, 2001; Mannstein et al., 2000]. A refined method and additional data resulted in a mean cover of 0.75% over Central Europe (8°W-23°E, 42°-56°N), see Figure 7.11 [Meyer et al., 2001; Mannstein et al., 2000]. The night-time contrail coverage in that region is approximately one third compared to that of daytime cover, in rough agreement with traffic variations.

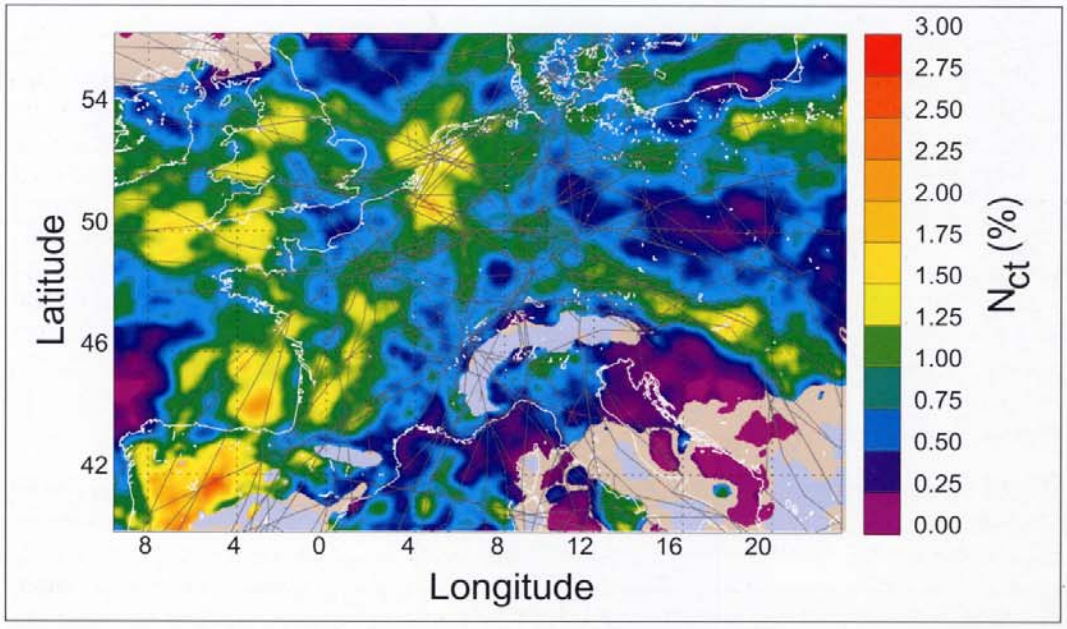

Figure 7.11 *Contrail cover (percentage of area covered with contrail cirrus) over Europe from NOAA-14 noon scenes for March 1995-February 1997. The lines indicate main traffic routes over Europe at 10-13 km altitude, between 1000 and 1300 UTC [Meyer, 2000].*

Analyses of satellite images have provided the contrail cover for a limited number of geographical areas only: Central Europe [Mannstein et al., 1999; Meyer et al., 2001], Eastern North Atlantic [Bakan et al., 1994], New Zealand (just 40 scenes) [Meyer, 2000], Indonesia [Mannstein et al., 2000], near Hawaii (case-studies) [Duda et al., 2001], and North America [Palikonda et al., 1999; Minnis et al., 2000]. Similar observation analyses are still missing for the main traffic routes over the Atlantic and Pacific.

To reach a global distribution of contrail cloud cover, Sausen et al. [1998] used ECMWF temperatures and humidity data, and an aircraft fuel inventory for present-day traffic providing the amount of fuel used in a grid point during persistent contrail conditions. The product was normalised to the remotely observed contrail cover in the region west of Europe based on the results of Bakan et al. [1994], which were the only published data available at that time. For fuel consumption as in 1991/1992, the calculated global averaged contrail cover amounts to 0.087% or about 0.1%, but values exceeding 5% can occur in the main air routes. As noted in Gierens et al. [1999a], the computed 1992 contrail cover is five times smaller (0.02% instead of 0.1% globally) if the observations of Mannstein et al. [1999] are used, which include the smaller night-time values in the daily mean value (0.5% daytime and one third for night-time cover over Central Europe), instead of those from Bakan et al. [1994] for normalisation. This would imply an important reduction relative to the assessment given in IPCC [1999].

The potential contrail cover is much greater. If aircraft were to fly everywhere and at all times the global average contrail cover (partially overlapping with cirrus clouds) could approach 16% [Sausen et al., 1998]. Over Europe this predicted value would be 12%, which is consistent with estimates derived from satellite observations [Mannstein et al., 1999] and *in situ* humidity measurements [Gierens et al., 1999a, 2000] using data from the MOZAIC project [Marenco et al., 1998; Helten et al., 1998]. If these numbers were realised it would mean a very large change in high cloudiness. The mean cirrus cover at northern mid-latitudes is about 20-30% according to different observations [Wang et al., 1996; Wylie and Menzel, 1999]

A diagnostic study of the global distribution of contrails using future air traffic scenarios in the years 2015 and 2050 was conducted by Gierens et al. [1999a], see Figure 7.12 (top part). They computed that the mean contrail cover could reach 0.25% in 2015 and between 0.26% and 0.75% in 2050 depending on the scenario for the increase in air traffic. To some extent the increase in contrail cover is stronger than for total fuel use alone, partly due to more efficient engines. While the estimates by Gierens et al. [1999a] were for a static climate, Sausen et al. [2000] considered a changing climate when estimating the fractional contrail cover. They found smaller values than Gierens et al. [1999a], mainly due to less contrail formation in a warmer climate in the future from the increase in greenhouse gases. For 1992, 2015, and 2050, they got 0.070, 0.16, and 0.30%, i.e., the changing climate (warming troposphere) results in a slower increase in contrail coverage. (The differences for 1992, 0.070% instead of 0.087%, result from the different temperature and humidity fields in the ECMWF analyses and the climate model computations.)

For the future, aircraft driven by liquid hydrogen are being discussed [Klug and Ponater, 2000]. Such aircraft would cause contrails over a larger range of altitudes than kerosene driven aircraft [Schumann, 1996]. The main reason for this is that the emission of water vapour mass is 2.5 times that of conventional fuel for the same energy content. The potential contrail cover would be about 50% larger if the aircraft were driven by liquid hydrogen instead of kerosene, see Figure 7.12 [Marquart et al., 2001]. Because of a cleaner exhaust with fewer particles available to form crystals, the contrails would be optically thinner if cryogenic fuels were to be used instead of kerosene [Ström and Gierens, 2001].

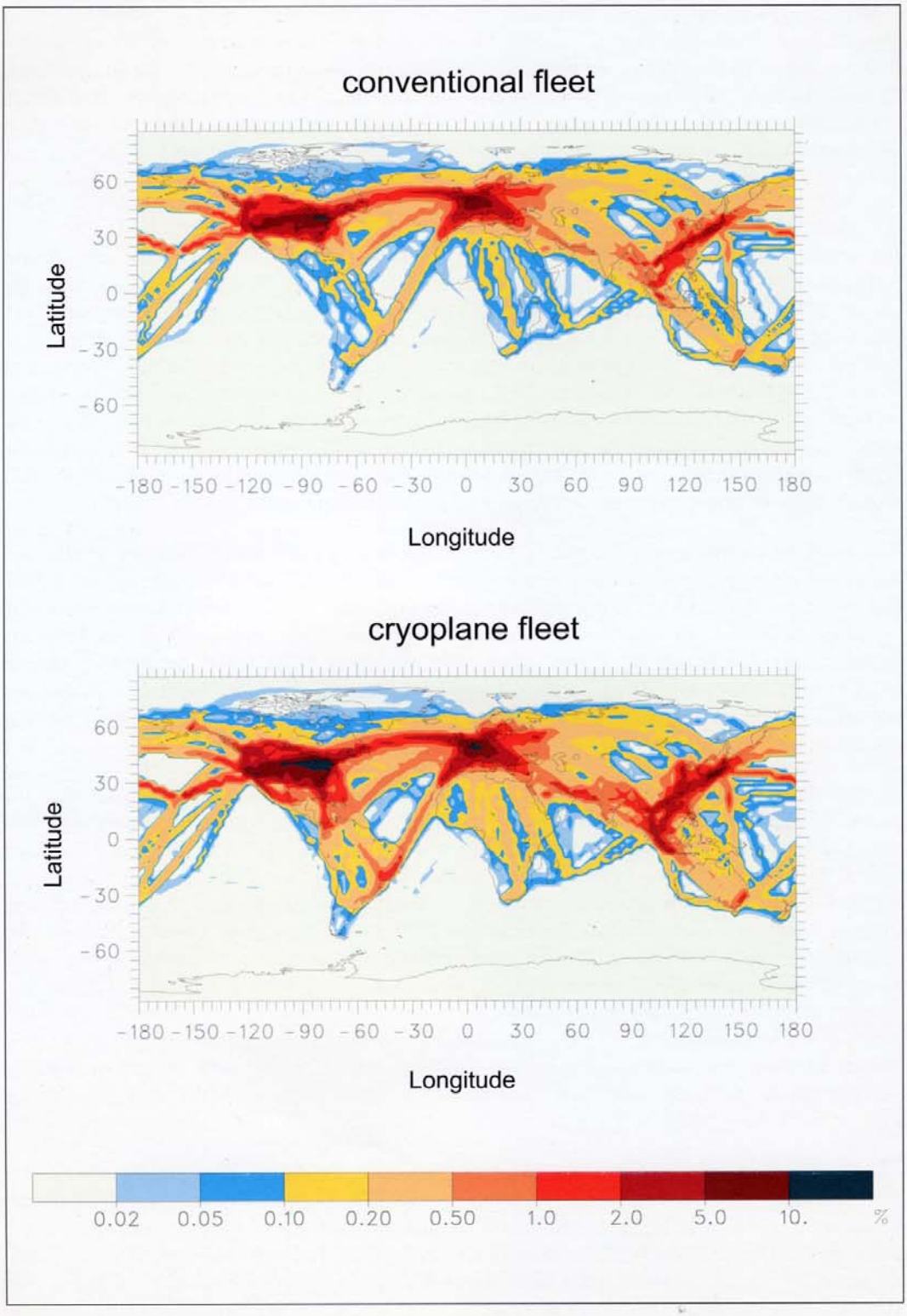

Figure 7.12 *Annual mean contrail area coverage (%) for a conventional fleet (top panel) and a hypothetical cryoplane fleet (bottom panel) in 2015. [Marquart et al., 2001].*

Contrail Indirect Effect

Contrail cirrus has been observed to form by transition of persistent contrails into cirrus clouds [Schumann and Wendling, 1990; Schumann, 1994, 2001; Minnis et al., 1998]. There is a potential for aerosol particles emitted by aircraft, or other anthropogenic sources, to induce changes in threshold conditions for cirrus formation and dissipation, or alter the crystal size distribution of natural clouds. This effect may occur at a place and time very different from where the emissions were released. But clear evidence for this effect is missing.

Wind shear and turbulence distort the linear signature of young contrails, which eventually become indistinguishable from natural cirrus. For this reason, estimates based on methods relying on the detection of linear clouds represent a lower limit for the additional cloud cover caused by aircraft emissions. Boucher [1999] analysed ground-based cloud observations between 1971 and 1991. The mean global increase in cirrus occurrence frequency per decade was 1.7% over land and 6.2% over ocean. The change in cirrus occurrence by region (300 km×300 km) shows a strong relation to aviation fuel used above 8km altitude, Figure 7.13. In regions with heavy air traffic the change per decade exceeded 5%. Several sets of

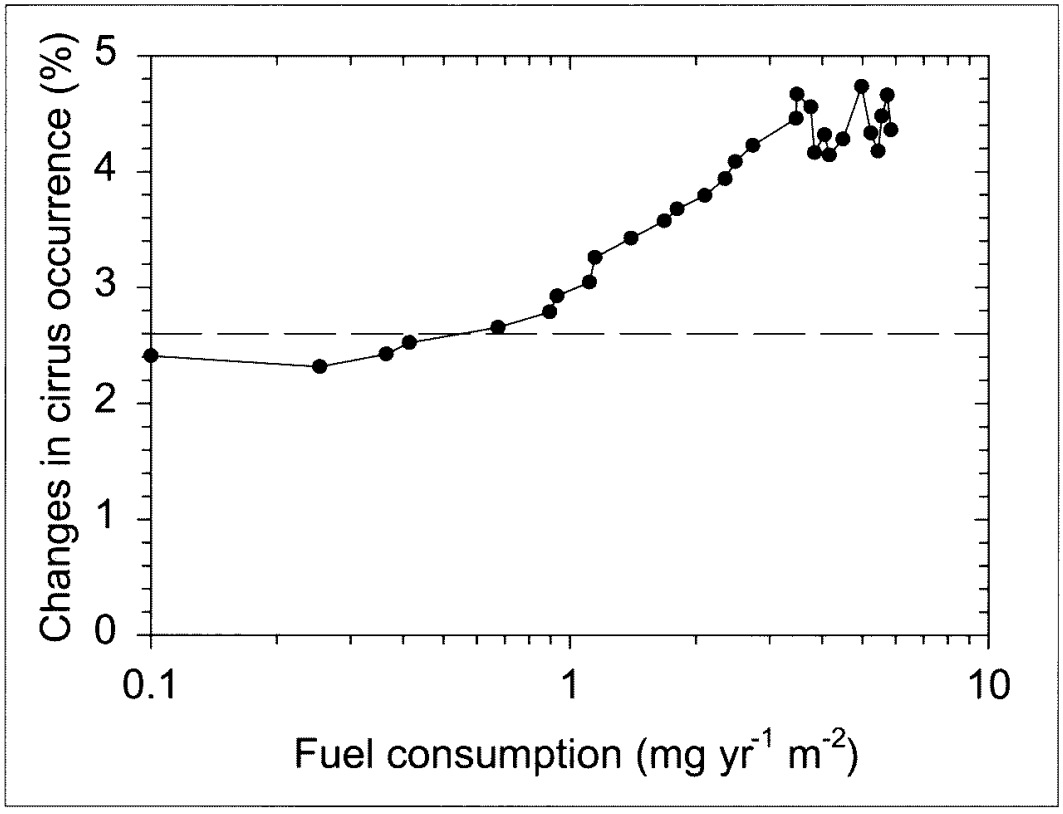

Figure 7.13 *Cirrus increase observed over North Atlantic over the years 1986-1990 relative to the years 1980-1985 versus aviation fuel consumption (dots with full line) in individual latitude-longitude grid boxes of size 3°×3° (plotted with data as in O. Boucher, see IPCC [1999]). The horizontal dashed line indicates the observed mean change in cirrus occurrence in the whole domain. The scatter at high fuel consumption is partially caused by the small number of data available in regions with high air traffic.*

satellite data have been used to compare trends in the contrail regions to other areas [IPCC, 1999]. The results show that the increase was 4 times larger (1.0-5.8, depending on the specific data set) in the regions with dense air traffic compared to elsewhere, and the deduced increase in high cloud cover was about 3 times larger than the computed linear-contrail cover [Minnis et al., 2001]. On the other hand, eleven years of HIRS cloud statistics reveal that high clouds increased until 1993 and then gradually decreased back to 1989 levels [Menzel et al., 2000], different from analysis of the same type of data for shorter periods [Wylie and Menzel, 1999]. Hence, any trend analysis from a short time period may be misleading.

The initial number density of ice crystals formed in cirrus is determined by the peak RH and depends strongly on the updraft velocity and on temperature [Kärcher and Lohmann, 2001]. The crystal number density results from the competition between generating supersaturation in the updraft and reducing supersaturation by vapour deposition on the growing ice particles. The number of ice particles increases with updraft speed. Modelling studies indicate that the peak RH is only a few percent larger than the freezing threshold RH, except for strong updraft speeds. In the case of homogeneous freezing of super-cooled aerosols, the number of crystals formed is found to be fairly insensitive to the number and size of available aerosol particles. According to model studies, about ten times more aerosol particles are required to increase the crystal number density by a factor of two [Jensen and Toon, 1994; Lin et al., 1998].

Ice nucleation can take place heterogeneously on suitable particles as soon as ice saturation is reached, but many recent observations of RH in the tropopause region, as shown for instance in Figure 7.9, often find ice supersaturated regions in seemingly cloud free air [Gierens et al., 1999b; Ovarlez et al., 1999, 2000; Jensen et al., 2001]. The data points partly cluster along lines of constant water concentration and partly along lines of constant temperature, indicating different reasons for RH variations. In some cases the RH values even approaches liquid saturation. Jensen et al. [2001] show that in cases with lack of effective ice nuclei (less than 0.01 cm^{-3}) the humidity will continue to rise in ascending air parcels and approach saturation with respect to liquid water unless the vertical motion is very slow. For slow ascent, immersion freezing and contact freezing of small water drops may become important mechanisms.

Jensen and Toon [1997] showed that, based on numerical simulations, aircraft emissions may change the cloud properties if the air contains more aircraft induced ice nuclei than crystals that would form through homogeneous nucleation in the absence of these ice nuclei. At temperatures below about -40°C, homogeneous nucleation or freezing of solution drops becomes the dominant mechanism. However, there is at the moment no consensus on the exact nature of cirrus formation. Bulk and size-resolved cirrus process models show large differences even when applied to idealised cases with prescribed ambient conditions (see GEWEX-cirrus modelling initiative, http://eos913c.gsfc.nasa.gov/gcss_wg2/) [Lohmann et al., 2000; Heymsfield and Iaquinta, 2000].

Ström and Ohlsson [1998a] observed enhanced crystal number densities in regions where the cloud particles contained elevated levels of absorbing material. The absorbing material appears to originate from exhaust soot emitted by aircraft. Typically the crystal density was enhanced by a factor of two in the "dirty" or perturbed regions of the cloud compared to the non-perturbed regions. Kristensson et al. [2000] compared the effective diameter in perturbed and non-perturbed cirrus, by stratifying the data according to the amount of absorbing material found in the crystals as in Ström and Ohlsson [1998a]. The results show that for temperatures below -30°C the effective diameter was reduced by 10-30% in the perturbed cirrus, see Figure 7.14. The radiative perturbation caused by such a change in the microphysical properties is potentially large [Wyser and Ström, 1998; Meerkötter et al., 1998].

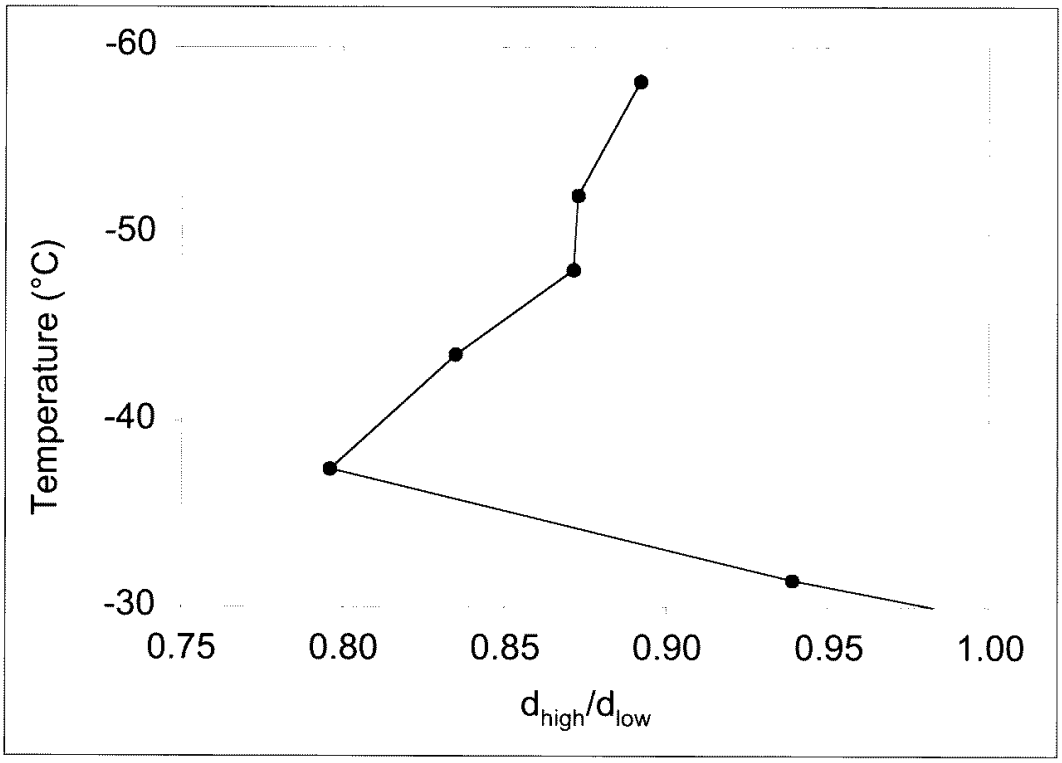

Figure 7.14 *The ratio of effective crystal diameters in regions with high (>0.01 μg m^{-3}) and low soot concentrations (d_{high}/d_{low}) versus temperature. [adapted from Kristensson et al., 2000].*

As clouds in general impact photodissociation of gas-phase species [Krol and Van Weele, 1997; Pfister et al., 2000], a similar impact might be expected from contrails. However, the effect of contrails on photochemistry has not yet been quantified.

Regional Aerosol Changes by Aircraft Emissions

The vertical profiles of nanometer sized particles measured near the North Atlantic flight corridor during POLINAT 2 [Schumann, 1999] exhibit an enhancement of particles within the corridor. Measurements within, above, and below the corridor revealed a non-volatile aerosol enhancement of 3:1 at corridor altitudes [Paladino et al., 2000]. Observations during SONEX found enhancements in fine particles (>17 nm) by about 20% in the lower stratosphere [Kondo et al., 1999b]. In the North Atlantic upper troposphere, mean enhancements of total and non-volatile particles (>18 nm) from aviation emissions are calculated to be about 8% and 4%, respectively [Anderson et al., 1999b].

Several recent studies tried to determine the aviation contribution to these measured particle concentrations. Schröder et al. [2000a] provided a simple estimate of the concentration of particles from aviation using measured particle emission indices within and outside contrails, previous estimates of fuel emissions [Gardner, 1998], and various particle lifetimes of 1, 3 or 7 days. The results are plotted in Figure 7.15. The figure also contains the measured 10-percentile concentration values of aerosols >7 nm based on the measurements of Schröder

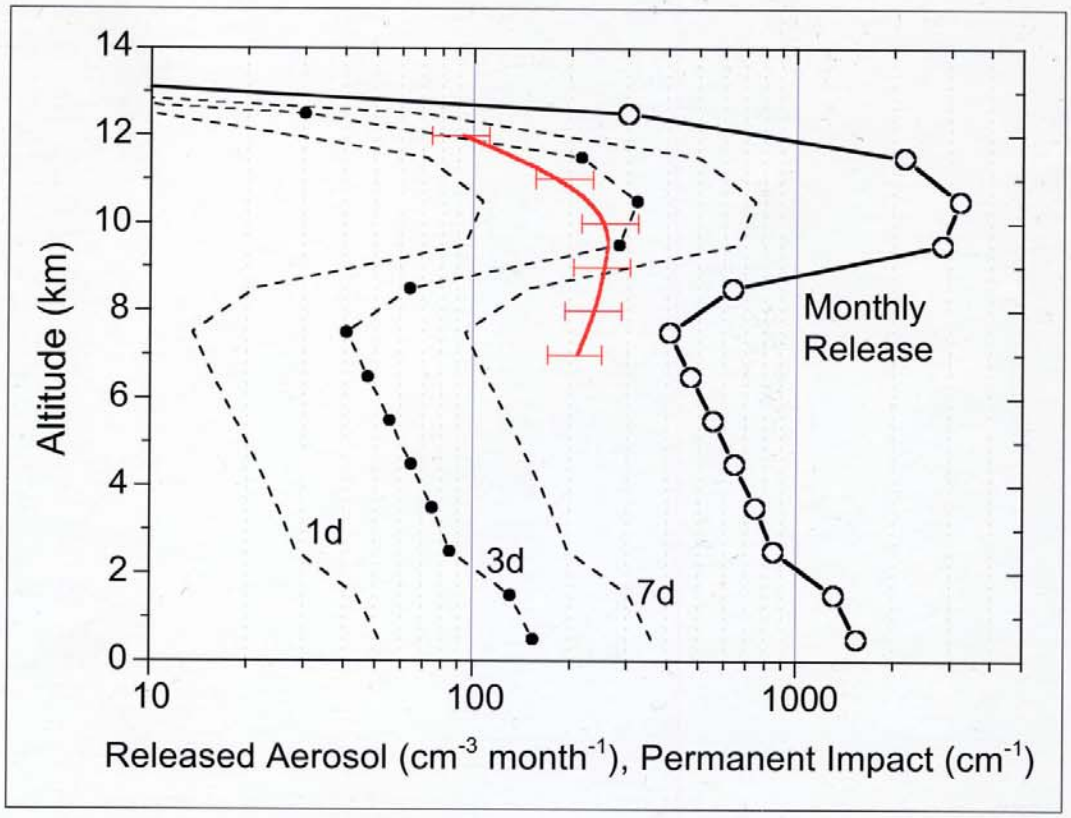

Figure 7.15 *Calculated aviation induced particle concentration in the NH mid-latitude atmosphere versus altitude: Measured 10-percentile concentration values per cm^3 and computed concentration increase due to aviation emissions for 1, 3, and 7 days lifetime [Schröder et al., 2000a]. Open circles: Total monthly aerosol release in cm^{-3} $month^{-1}$. Dashed lines: Resultant particle concentrations from aviation in cm^{-3} for 1, 3 and 7 days lifetime. Bold line with error bars: Measured 10 percentile concentration values in cm^{-3} (error bars indicate 20% uncertainty) of aerosols >7 nm, based on statistics over 4×10^4 measurements. [Schröder, 2000].*

and Ström [1997] for the summer tropopause region over Central Europe. The 10-percentile values represent the lowest concentration to be expected at any time. Since aviation emissions are present permanently, their contributions must stay below the 10-percentile value. Consequently, a lifetime of 1-2 days for the aircraft emissions in this region and a maximum of 100-200 cm^{-3} particles as permanent aviation signature would be roughly consistent with the observations in the altitude range between 9 and 12 km.

These findings are consistent with computations by Schlager et al. [1997], Kärcher and Meilinger [1998], Danilin et al. [1998], and observations by Hofmann et al. [1998]. Jäger et al. [2000] derived enhanced optical depth values (0.005-0.02) in the height range of air traffic (8-13 km) from lidar measurements (532 nm) over Garmisch, Germany, for 1997 and 1998, at a time when the influence of the Pinatubo aerosol had ceased.

Only a few model studies have yet considered the concentration change of aerosols due to subsonic emissions [Danilin et al., 1998; Kjellström et al., 1999]. In a global stratospheric and tropospheric sulphate aerosol model, subsonic aircraft were found to contribute about 3% to the

total aerosols mass in the stratosphere and 20% of the surface area density at 14 km altitude north of 45°N [Pitari and Mancini, 2000; Pitari et al., 2001b].

In principle, aircraft may contribute to the formation of polar stratospheric clouds (PSCs) of type 1b (liquid), composed of super-cooled ternary solutions of $H_2SO_4/HNO_3/H_2O$, or 1a (solid), presumably composed of nitric acid trihydrate (which is the stable nitric acid hydrate at stratospheric conditions). Furthermore, larger type 2 ice PSC particles form below the ice frostpoint temperature. The heterogeneous chemical reactions taking place on the surface of PSC particles, activating halogen species, depend on the chemical composition and physical phase of the particles. In addition, only solid type PSC particles are responsible for denitrification and dehydration, i.e. the irreversible removal of reactive nitrogen and water by gravitational sedimentation of nitric acid holding particles [DelNegro et al., 1997; Larsen and Knudsen, 2000].

Model studies by Danilin et al. [1998] indicate that subsonic aviation has a very small impact on water vapour concentrations in the stratosphere and do not increase PSC occurrence to any important degree. Results obtained within AEROCHEM II considered subsonic and combined subsonic/supersonic fleet scenarios for the year 2015. The results indicate that emissions from subsonic aircraft only cause minor influence on PSC occurrence and surface area densities. However, the effects from a combined fleet of subsonic and supersonic aircraft clearly show up in model simulations. Increased concentrations of HNO_3 and H_2O from supersonic aircraft on the order of 5-10% will have a direct influence on the thermodynamic threshold temperatures for the existence of particles containing nitric acid trihydrate, super-cooled ternary solutions and ice in the northern hemisphere polar stratosphere [DelNegro et al., 1997]. This may increase the frequency of occurrence of temperatures below these thresholds by 2-5% and increase the type 1b PSC equilibrium volumes by about 10% [Larsen and Knudsen, 2000].

Heterogeneous Chemical Processes

Aircraft emissions may contribute to some reduction of ozone by heterogeneous chemistry in the lowermost stratosphere, but direct evidence for this effect is missing. Heterogeneous chemistry involving reactions in aerosol particles and cloud droplets in the lower stratosphere and in the troposphere may affect O_3 concentrations in a number of ways including production and loss of HO_x and NO_x, direct loss of O_3, and production of halogen radicals [Jacob, 2000]. Several papers suggest that heterogeneous effects are expected to occur on ice particles [Borrmann et al., 1996, 1997; Hendricks et al., 1999, 2000; Meilinger et al., 2001; Solomon et al., 1997]. Hypotheses regarding fast O_3 loss on soot or in clouds, and fast reduction of HNO_3 to NO_x in aerosols in the atmosphere are not yet supported by evidence. Heterogeneous reactions on soot surfaces are too slow to cause measurable ozone changes [Gao et al., 1998; Kamm et al., 1999; Longfellow et al., 2000]. There remains significant uncertainty in the role that heterogeneous chemistry on ice particles exerts on NO_x. Some observation suggest the presence of subvisible cirrus in the lower stratosphere just above the tropopause [Gierens et al., 1999a; Kärcher and Solomon, 1999; Lelieveld et al., 1999a; Solomon et al., 1997; Wang et al., 1996], while other studies insist that such cases are limited to a narrow layer above the thermally defined tropopause [Jensen et al., 2000; Smith et al., 2001a].

Previous studies concentrated on the heterogeneous chemistry of the ozone layer. A few recent models have also studied the tropopause region. These studies indicate that the heterogeneous chemistry on visible cirrus or even sub-visible ice clouds may induce ozone losses of a few

percent in the entire tropopause region, in particular in summer [Bregman et al., 2000a, 2001; Meilinger et al., 2001; Pitari et al., 2001b, 2001c; Solomon et al., 1997]. Observations indicate possible chemical ozone loss associated with tropical cirrus clouds [Roumeau et al., 2000]. At present, little observational evidence exists for heterogeneous chemical effects on cirrus in the mid-latitude tropopause region [Keim et al., 1996; Lelieveld et al., 1999a]. Observational data of inorganic chlorine and bromine compounds in the tropopause region are only sparsely available [Arnold and Spreng, 1994; Lelieveld et al., 1999a]. Models rely mostly on computed Br_y and Cl_y concentrations [Borrmann et al., 1997; Hendricks et al., 1999]. These models do not account for the fact that cirrus clouds in the lower stratosphere probably result from transport of humid tropospheric air masses into the lower stratosphere [Zahn et al., 2000], hence they contain low amounts of inorganic chlorine [Solomon et al., 1997]. Very recently, Smith et al. [2001a] report on ClO measurements in the lowermost stratosphere. They find that the ClO concentration is in most cases below 10 pmol/mol and hence is too low to cause significant ozone destruction. They suggest that mid-latitude ozone loss is not controlled in situ by the mechanism of cirrus cloud and/or cold aerosols enhancement of chlorine radicals in the vicinity of the tropopause.

It should be noted that the studies above discuss ozone losses due to natural cirrus clouds. Evidence for aviation-induced aerosol impact on ozone is missing. Only a few studies address this topic explicitly [Kärcher and Meilinger, 1998]. Computations with an expanding plume model with chemistry have shown that contrails forming at ice supersaturated ambient air conditions and cirrus particles provide enough surface for heterogeneous chemistry to reduce the O_3 increase, which is computed for pure gas chemistry, by activation of chlorine compounds [Kraabøl and Stordal, 2000]. In plumes too dry to form contrails, the impact of heterogeneous reactions was found to be negligible [Kärcher, 1999; Schumann et al., 2000a]. The heterogeneous chemistry may enhance the importance of ozone formation by NO_x emissions because NO_x emissions bind part of the activated halogen radicals and hence reduce ozone loss otherwise resulting from heterogeneous chemistry, as shown for bromine chemistry by Hendricks et al. [2000]. Ice particles may also act as a sink for HCl and HBr. Any heterogeneous chemistry effects from aviation induced contrail cirrus would be much smaller than that from cirrus simply because they are less frequent.

7.3.3 Transport of gases and particles in the upper troposphere and lower stratosphere

The concentration of gases and particles emitted or formed through secondary processes from subsonic aircraft during cruise in the upper troposphere or lower stratosphere is largely controlled by transport mechanisms in the tropopause region. Models show large differences in the computed concentrations and residence times of species in the tropopause region, mainly because of differences in wind and turbulence fields, grid resolution, and numerical schemes used for calculating advection. The maximum concentration of a tracer representing the combustion products by aviation can be simulated with present models no better than within a factor of 2 [Danilin et al., 1998; Rogers et al., 2000a].

Two-dimensional (2-D) models cannot resolve the three-dimensional (3-D) structure of stratosphere-troposphere exchange. They describe transport of species using wind fields and turbulent diffusivities which tend to underestimate the mixing process of local emissions. Therefore downward mixing of a tracer emitted at cruise altitude at mid latitudes is more efficient in 3-D than in 2-D models [Rood et al., 2000]. The models suffer from coarse numerical resolution [Velthoven and Kelder, 1996], imperfect meteorological input data [Bregman et al., 2000b], and from approximation errors of the numerical schemes used. Off-

line global chemical transport models (CTMs, such as the OSLO-CTM2 [Berntsen et al., 2000]), can use meteorological data from ECMWF at typically T63 resolution (triangular truncation at wave number 63; corresponding to 1.875°×1.875°) with 19-31 levels up to 10 hPa. A realistic description of the local and instantaneous transport of air and its constituents across the tropopause requires a resolution of at least 1°×1° [Siegmund et al., 1996]. However, due to limited computer resources most simulations are done with coarser (T21-T42) resolution. Rogers et al. [2000b] show that inter-annual variations in meteorology cause changes in O_3 perturbations due to supersonic aircraft emissions which are of a magnitude similar to the differences between O_3 perturbations calculated by models within IPCC [1999]. The inter-annual variability of the strength of the meridional circulation in the upper troposphere and lower stratosphere, as diagnosed from ECMWF reanalyses for the period 1979-1993, is about 10%; a systematic trend during this period is not observed [Siegmund, 2001]. Some recent models used Lagrangian transport schemes to avoid numerical diffusion [Reithmeier and Sausen, 2000; Schoeberl and Morris, 2000; Stevenson et al., 1997]. General circulation climate models often suffer from simulating a too high and cold tropopause [Gates et al., 1999]. The problem may be overcome partly by enhancing the vertical resolution, in particular near the tropopause, e.g., from 19 to 39 levels in the ECHAM4 global circulation model (GCM) [Land, 1999]. Some differences are caused by different assumptions in the construction of emissions inventories. It is very important to place the correct fraction of emissions above the tropopause in the model [Gettelman and Baughcum, 1999].

In simulations of secondary species formed or affected by aircraft emissions (e.g., O_3, CH_4, HNO_3) difficulties to simulate the vertical transport by convection in the troposphere, wash-out, photolysis rates, lightning source, and chemical conversion, add to differences between models [Berntsen et al., 2000; Grewe et al., 2001a; Meijer et al., 2000]. The rapid vertical mixing by convection has a large impact on the background concentration of NO_x in the upper troposphere, thereby affecting the non-linear ozone production efficiency of NO_x emissions from aircraft [Berntsen and Isaksen, 1999]. Convection also effectively transports the ozone produced to lower altitudes with faster ozone loss to the surface.

Whereas models that simulate subsonic aviation effects have to provide high resolution near the tropopause and the lower stratosphere, model studies of supersonic aviation have to resolve the whole stratosphere below about 1 hPa [Steil et al., 1998; Manzini and Feichter, 1999]. Timmreck et al. [1999b] showed that a higher vertical resolution at the tropopause (~700 m) is essential for the modelling of realistic lower stratosphere residence times, whereas the model top only has small impact on the residence times. Recently, interactively coupled climate-chemistry models have been developed. These models enable simultaneous treatment of meteorology and chemistry, and account for the radiative impact of changing greenhouse gases (O_3, CH_4, N_2O, etc.) on dynamics [Dameris et al., 1998a, 1998b; Grewe et al., 1999, 2001b; Hein et al., 2001; Roelofs and Lelieveld, 2000; Schnadt et al., 2001].

Model studies performed within the projects AERONOX, AEROCHEM, POLINAT, MOZAIC, and TOPOZ and related national projects considered subsonic aircraft emissions and/or transport in the tropopause region by various approximations. Sausen and Köhler [1994] and van Velthoven et al. [1997] studied the distribution using a NO_x-like tracer with prescribed lifetimes, while Rogers et al. [2000a] focused on a tracer with longer lifetime. Kraus et al. [1996] and Köhler et al. [1997] simulated NO_x as a tracer with linearised conversion models. NO_x has also been studied as a component with a more complex chemistry cycle within CTMs [Wauben et al., 1997; Stevenson et al., 1997; Berntsen and Isaksen, 1999] or GCMs [Dameris et al., 1998b]. These studies show that the impact of upper tropospheric NO_x emitted from

subsonic aircraft in the upper troposphere is significant. Zonal mean aviation contributions of 20-70%, depending on season (largest in winter), to the NO_x concentration in the upper troposphere at 30°-60°N were computed. Other model studies partly find smaller contributions [EU, 1998; IPCC, 1999]. However, the scatter is surprisingly small when all model results are normalised to the same emission rates [IPCC, 1999].

Recently, CTMs have been integrated into numerical weather forecast systems to provide chemical forecasts [Flatøy et al., 2000]. These forecasts have been found extremely valuable for planning of aircraft measurements [Schlager et al., 1999].

7.3.4 Role of nitrogen oxides in changing ozone and methane concentration

Sources of NO_x and Expected Concentration

The global sources of NO_x have been compiled and reviewed by Lee et al. [1997b], see Table 7.4. Some of the sources, in particular those of lightning [Huntrieser et al., 1998, 2001; Höller et al., 1999; Bradshaw et al., 2000; Lelieveld and Dentener, 2000; Meijer et al., 2001], are still very uncertain, up to a factor of ten. The vertical profile of NO_x releases from thunderstorms and the relative source rates over oceans and land are approximated with large uncertainties [Grewe et al., 2001b]. Lightning NO_x emissions sustain the NO_x levels and the O_3 production required to explain the persistent ozone plumes emanating from biomass burning regions [Hauglustaine et al., 2001].

Previous studies assumed too small NO_x emission rates from aviation for past and present traffic, partly because of underestimates in the fuel consumption and partly because of too small emission indices. The NO_x emission inventories for aviation have been derived from world-wide traffic data, performance data of individual aircraft/engine combinations and emission factors estimated for specific engines [Gardner et al., 1997]. For a recent study of aircraft emissions of NO_x over China see Ma and Zhou [2000]. The total aviation NO_x emissions may be roughly estimated from the global aviation fuel consumption and the mean emission index of NO_x from aircraft. The fleet averaged NO_x emissions values in previous emission inventories [IPCC, 1999] range from 12-14 g/kg. Emissions measured behind large cruising airliners [Schulte et al., 1997] and discussions of various sources of errors [IPCC, 1999; Daggett et al., 1999] suggest that the larger value is more appropriate. Therefore, for 2000, a best estimate for the amount of NOx emissions from aircraft engines in global (civil and military) aviation is 0.9 (0.7-1.0) Tg(N)/yr (Table 7.4).

The resultant relative contributions of the NO_x emission to the NO_x concentration at 30-60°N, 9-11 km altitude has been computed in several model studies with different results. The relative contributions listed in Table 7.4 serve as a rough guide.

Recent Measurements of Trace Species Near Air Traffic Corridors

Until recently, very little observational NO_x data were available to check model computations in the North Atlantic region [Drummond et al., 1988; Weinheimer et al., 1994; Emmons et al., 1997, 2000; Rohrer et al., 1997a; Thakur et al., 1999; Bradshaw et al., 2000]. The first measurements of aircraft emissions in subsonic aircraft plumes and in the North Atlantic flight corridor were performed within the German research project "Pollutants from Air Traffic" ("Schadstoffe in der Luftfahrt") [Arnold et al., 1992; Klemm et al., 1998; Rohrer et al., 1997b;

Schlager et al., 1997; Schulte and Schlager, 1996; Schumann et al., 1995; 1997; Slemr et al., 1998, 2001; Ziereis et al., 1999].

Systematic NO_x measurements were made from May 1995 to May 1996 within the Swiss Nitrogen Oxides and Ozone along Air Routes (NOXAR) project [Brunner, 1998; Brunner et al., 1998; Dias-Lalcaca et al., 1998] and within the POLINAT and the SONEX experiments [Singh et al, 1999; Thompson et al., 2000; Schlager et al., 1999; Schumann et al., 2000a]. The projects NOXAR, SONEX, POLINAT, and MOZAIC considerably extended the database of distribution of NO_x, O_3, H_2O, and other trace gases in the tropopause region at northern mid-latitudes, in particular over the North Atlantic. Between 1994 and 1998, the POLINAT and STREAM projects measured the composition of the atmosphere from the mid-troposphere to lowermost stratosphere. The data included atmospheric state parameters, mixing ratios of O_3, H_2O, CO_2, CO, $(CH_3)_2CO$, SO_2, HNO_3, NO, NO_2, NO_y, and aerosol number size distributions [Schumann et al., 2000a]. The ongoing MOZAIC III project will provide new data on NO_y. Plots of NO, NO_x and O_3 mixing ratios at 10-12 km altitude (and others) based upon measurements made during various projects including NOXAR, POLINAT 1 and 2, and SONEX, are available on the internet (http://aoss.engin.umich.edu/SASSarchive/). Figure 7.16 shows, for example, the NO_x distribution in the altitude range of cruising aircraft.

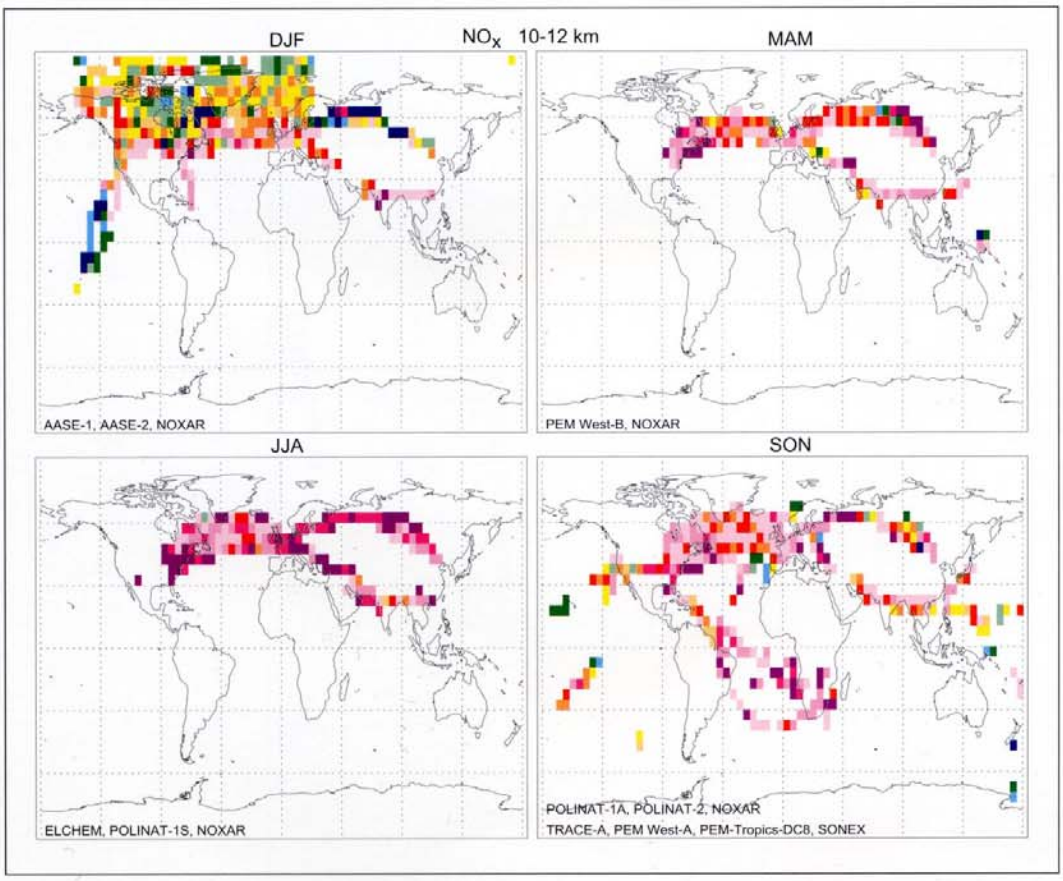

Figure 7.16 *NO_x mole fraction in various regions of the globe as obtained from recent in situ measurement projects in the altitude range 10-12 km for four seasons. [Emmons, 1999].*

Near the North Atlantic air traffic corridor, the vertical NO, NO_x, and NO_y profiles obtained within POLINAT show local maxima near 10.5-11.5 km altitude, see Figure 7.17. The mean values of measured NO concentrations are rather large and vary between 0.1 and 0.14 nmol/mol in summer and 0.03 and 0.1 nmol/mol in late autumn [Ziereis et al., 1999, 2000a]. The local maxima occur at the altitudes of major air traffic levels, regardless of whether the air mass is of tropospheric or stratospheric origin. More than 64% of the observed NO_x is made up of NO, and more than 25% of the NO_y is NO_x in the altitude range from 10.5-11.5 km. The large NO/NO_x ratio reflects the strong NO_2-photolysis rate, and low temperature and still rather low O_3 mixing ratio at these altitudes [Schlager et al., 1997; Ziereis et al., 1999]. The large NO_x/NO_y ratio indicates a large fraction of fresh NO_x emissions.

The measurements performed aboard the B-747 during NOXAR and POLINAT 2 provided a representative picture of O_3 and NO_x concentrations in the flight corridor, see Figure 7.18. At cruise altitudes (300-190 hPa, 9.2-12.1 km) the NO_x concentrations obtained between September and November in the years 1995 and 1997 were very similar and ranged from 0.1 to 0.15 nmol/mol over the North Atlantic (40-60°N and 10-40°W) and from 0.19 to 0.28 nmol/mol above the continental United States of America (30-60°N and 60-90°W) [Jeker et al., 2000]. The NO_x abundance measured onboard the B-747 shows mixing ratio values versus flight time with many short-period (3-30 s) peaks often exceeding 3 nmol/mol, obviously from aircraft emissions, and wider peaks exceeding 0.5 nmol/mol (often above 1 nmol/mol) over more than 500 km distance, reflecting contributions to the upper troposphere by convection of polluted boundary layer air masses or lightning.

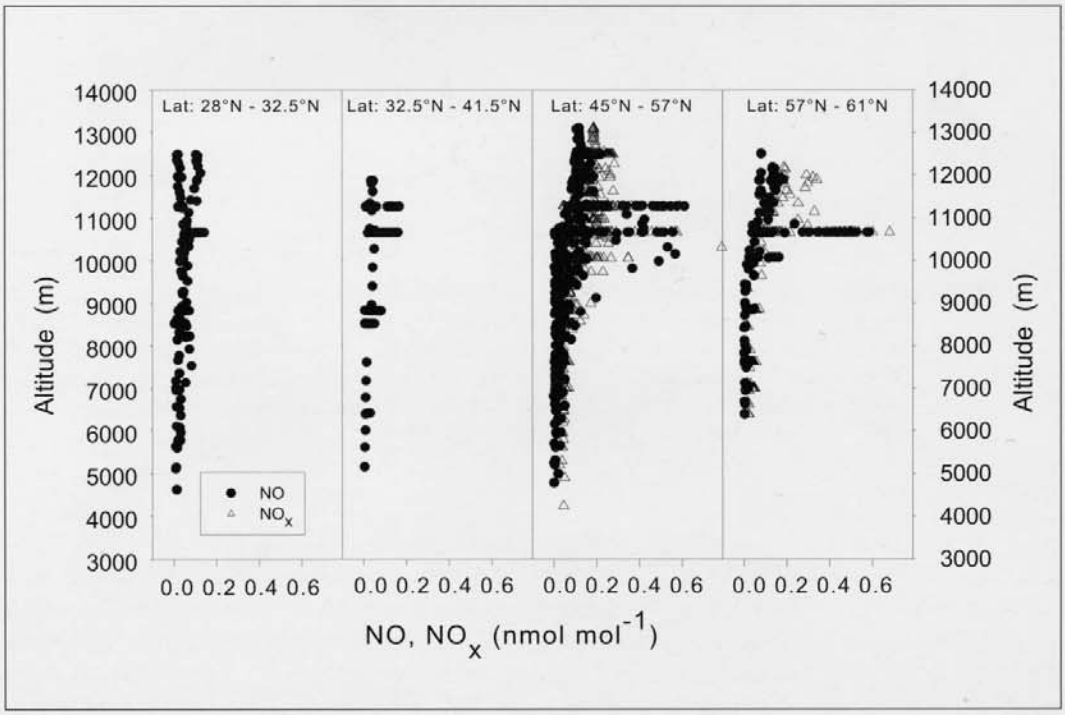

Figure 7.17 *NO and NO_x volume mixing ratios observed during POLINAT 2 in September and October 1997. The data have been divided in four latitude bins as indicated. All volume mixing ratios given represent 1 min averages. [Ziereis et al., 2000a].*

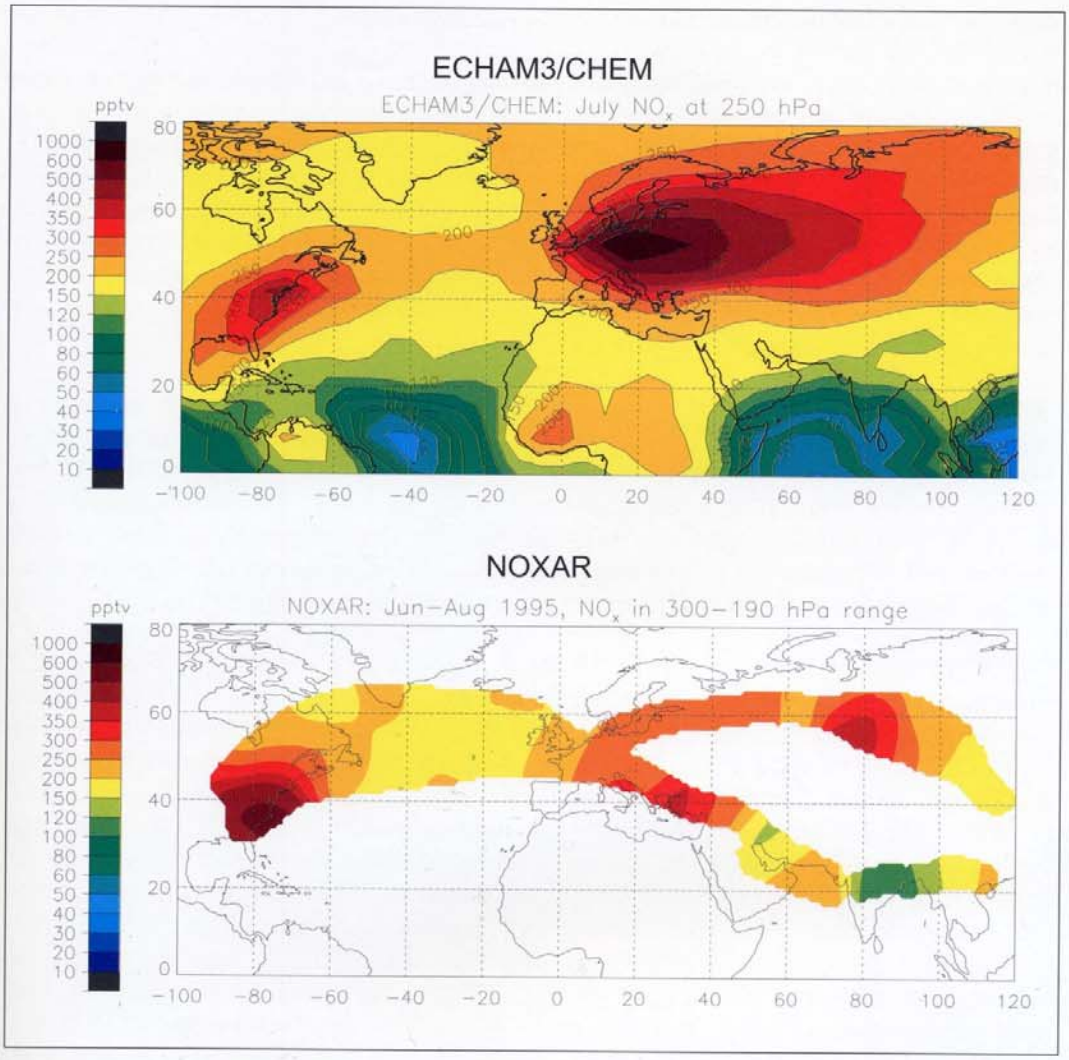

Figure 7.18 *Daytime NO_x concentration distribution versus latitude and longitude at cruising altitude in the range of the Swissair B-747. The top panel shows the ECHAM3/CHEM model results at 250 hPa. The bottom panel shows the NOXAR measurements with 2 min averaged samples taken at 190-300 hPa from June-August 1995. The colour coding ranges from 0 (black, followed by blue) to more than 1000 pptv (dark red and black). Data from Brunner [1998] and Grewe et al. [2001a], figure from Schumann et al. [2000a].*

Figure 7.18 shows the NOXAR and POLINAT results compared with model output from CTMs and the ECHAM/CHEM global circulation chemistry model [Brunner, 1998; Brunner et al., 1998; Grewe et al., 2001a; Schumann et al., 2000a; Ziereis et al., 1999]. The model results agree with the measured data within a factor of about two, but do not resolve the observed small scale variability. A comparison of various CTMs with ozone measured from MOZAIC shows that models often fail to reproduce the observed high variability in the upper troposphere [Law et al., 2000]. It seems that far higher numerical resolution is required for to correctly model of the natural variability.

Regional Gas Concentration Changes by Aircraft Emissions

A unique tracer to follow aircraft emissions does not exist and the mean concentration values of species are difficult to verify by measurements because of the large natural variability. Emissions from air traffic are clearly measurable by the increases in the concentrations of NO_x, HNO_2, HNO_3, SO_2, H_2O, particles and CO_2 observed within individual aircraft exhaust plumes [Arnold et al., 1992; Schulte et al., 1997; Schumann, 1997b; Schumann et al., 1998; Tremmel et al, 1998]. In the flight corridor, emissions give a very spiky signal resembling the superposition of several plumes, this is particularly noticeable for NO_x and particles [Schlager et al., 1997]. It takes about 3-10 hours before individual plumes get diluted to background NO_x concentration values within the range of background variance.

POLINAT 1 provided the first measurements that indicate an impact of aircraft emissions on the NO_x concentration field at regional scales. The measurements were taken under special weather conditions when the flight corridor extended through a stagnant anticyclone that was located above the British Islands more than seven days in June 1995. The measurements during this period show strong increases in NO_x over time. Model computations indicate that the observed NO_x increases can be explained only when including the aircraft emissions in the calculations [Meijer et al., 2000; Schlager et al., 1996; Schumann et al., 2000a].

The recent studies performed within POLINAT 1 and 2 and the NASA project SONEX provided indirect evidence, using combined model and measurement analysis, of a measurable regional increase in NO_x and particle concentration within or near the North Atlantic flight corridor. During POLINAT 2, two flights were dedicated to study a predicted high impact of aircraft emissions. The predictions were provided with a CTM in a prediction mode [Flatøy et al., 2000]. The measurements identified large scale enhancements of the NO mixing ratio inside the corridor of about 50-150 pmol/mol. These enhancements were attributed to aircraft emissions by means of simultaneous tracer measurements, back trajectory analyses, traffic distribution, and model predictions with and without aircraft emissions [Schlager et al., 1999]. Though the highest NO_x and NO_y values observed during SONEX were associated with lightning sources [Jeker et al., 2000; Singh et al., 1999], strong evidence was found that aircraft emissions contribute up to 0.13 nmol/mol or 20-70% to NO_x and 0.35 nmol/mol or 10-20% to NO_y near the North Atlantic flight corridor during SONEX and POLINAT 2 [Koike et al., 2000; Kondo et al., 1999b; Ziereis et al., 2000a]. Large NO_y concentrations have been measured in the lowermost stratosphere in the Arctic sub-vortex region, and may originate partly from aircraft emissions north of 60°N [Ziereis et al., 2000b].

A 3-D modelling study using SONEX/POLINAT 2 data concludes that aircraft emissions were clearly the dominant source for NO_x and responsible for about 50% of the observed NO_x in the upper troposphere (with a maximum of 250 hPa) [Meijer et al., 2000]. Surface emissions and lightning contribute about 15-25% to the NO_x abundance in the upper troposphere [Grewe et al., 2001a; Köhler et al., 1997; Meijer et al., 2000; Ziereis et al., 1999].

Predicted Ozone Changes

In the troposphere and in the lower stratosphere, ozone is produced by the photochemical oxidation of CO and HCs which is catalysed by NO_x and hydrogen oxide radicals HO_x. The production rate of O_3, $P(O_3)$ depends mainly on the abundance of HO_2 and NO. The ratio of HO_2 to OH decreases with increasing concentration of NO. Therefore, $P(O_3)$ increases with

NO, at least for low NO concentrations [Brasseur et al., 1996; Ehhalt and Rohrer, 1994; Faloona et al., 2000; Flatøy and Hov, 1996; Wennberg et al., 1998]. For NO_x concentrations at a threshold value between 0.1 and 0.4 nmol/mol, $P(O_3)$ is expected to reach a maximum. For larger NO_x concentrations, reactions of OH with HO_2, NO_2 and HNO_4 cause a reduction of OH and hence a reduction of ozone production. Hence, addition of NO_x from aircraft will increase or decrease $P(O_3)$ when the background NO_x concentration is below or above this threshold. Acetone ($(CH_3)_2CO$) and other carbonyls may increase the sensitivity of $P(O_3)$ to aircraft NO_x.

The NO_x concentration measured during SONEX and POLINAT in the North Atlantic flight corridor is still low enough to let any additional NO_x enhance O_3 production, in particular when accounting for the mixing of the NO_x emissions into the upper troposphere, where the NO_x concentration is often below 0.1 nmol/mol. SONEX observations [Jaeglé et al., 2000] indicate that the OH abundance and O_3 production may continue to increase with NO_x concentrations up to 1 nmol/mol (larger than about a factor of three than the calculated NO_x threshold concentration) because high NO_x concentrations were often associated with high HO_x sources. Calculations using a 3-D global CTM [Berntsen and Isaksen, 1997] and a 3-D GCM [Dameris et al., 1998b] indicate that the number of O_3 molecules produced per emitted NO_x molecule decreases by only about 30% even when the NO_x emissions from air traffic increases from 0.5 Tg(N)/yr (in 1992) to 3.46 Tg(N)/yr (the 'high 2050' case used in IPCC, 1999; Grewe et al., 1999; Isaksen et al., 2001].

Sources of HO_x include reactions of excited-state oxygen atoms, $O(^1D)$, with water vapour, oxidation of methane, and the photolysis of carbonyl and peroxide compounds (preferably acetone). The dependence of the rate of ozone production on the availability of H_2O, O_3, CO, $(CH_3)_2CO$, HO_x and other radical source gases [Singh et al., 1995] is the topic of several recent studies [Arnold et al., 1997b, 1997c; Grooß et al., 1998; Hauglustaine et al., 1998; Jaeglé et al., 2000; McKeen et al., 1997; Müller and Brasseur, 1999; Singh et al., 2000; Wennberg et al., 1998; Wohlfrom et al., 1999]. Brühl et al. [2000b] show that 1 nmol/mol of acetone may double aircraft-related ozone production; while PAN acts as a sink for NO_x and hence lowers ozone production. Hence, it is very important to know the concentration of these gases in the tropopause region in order to be able to assess the impact of NO_x emissions from aircraft on ozone.

Three-dimensional global [Berntsen and Isaksen, 1997; Dameris et al., 1998a, 1998b; Grooß et al., 1998; Meijer et al., 2000; Stevenson et al., 1997; Wauben et al., 1997] and regional CTMs [Flatøy and Hov, 1996; Hov and Flatøy, 1997] predict photochemical ozone generation due to present NO_x aircraft emissions on time scales of weeks, reaching equilibrium values of an order of 4-10% of background concentrations in the upper troposphere.

The estimated increase in the zonally averaged tropospheric ozone column (Dobson Units (DU)) due to aircraft NO_x emissions is in the range 2-6 DU in 2015 at northern mid- and high-latitudes during spring and summer seasons, see Figure 7.19. This enhancement is in the range of 20-50% of the enhancement of O_3 from all pollution sources since the pre-industrial time [Berntsen et al., 2000]. Note that the models have different vertical resolution, which impacts on the dynamical and chemical processes in the tropopause region, and use different chemical modules. ECHAM/CHEM is a fully coupled chemistry-climate model which explicitly considers stratospheric dynamics and chemistry; the O_3 response to NO_x from aircraft is strongly influenced by stratospheric dynamics, especially the meridional transport (towards the winter pole); the distribution of the response is similar to that of the total O_3 column and shows a spring maximum. The ULAQ (University of l'Aquila) model uses a coarser resolution than

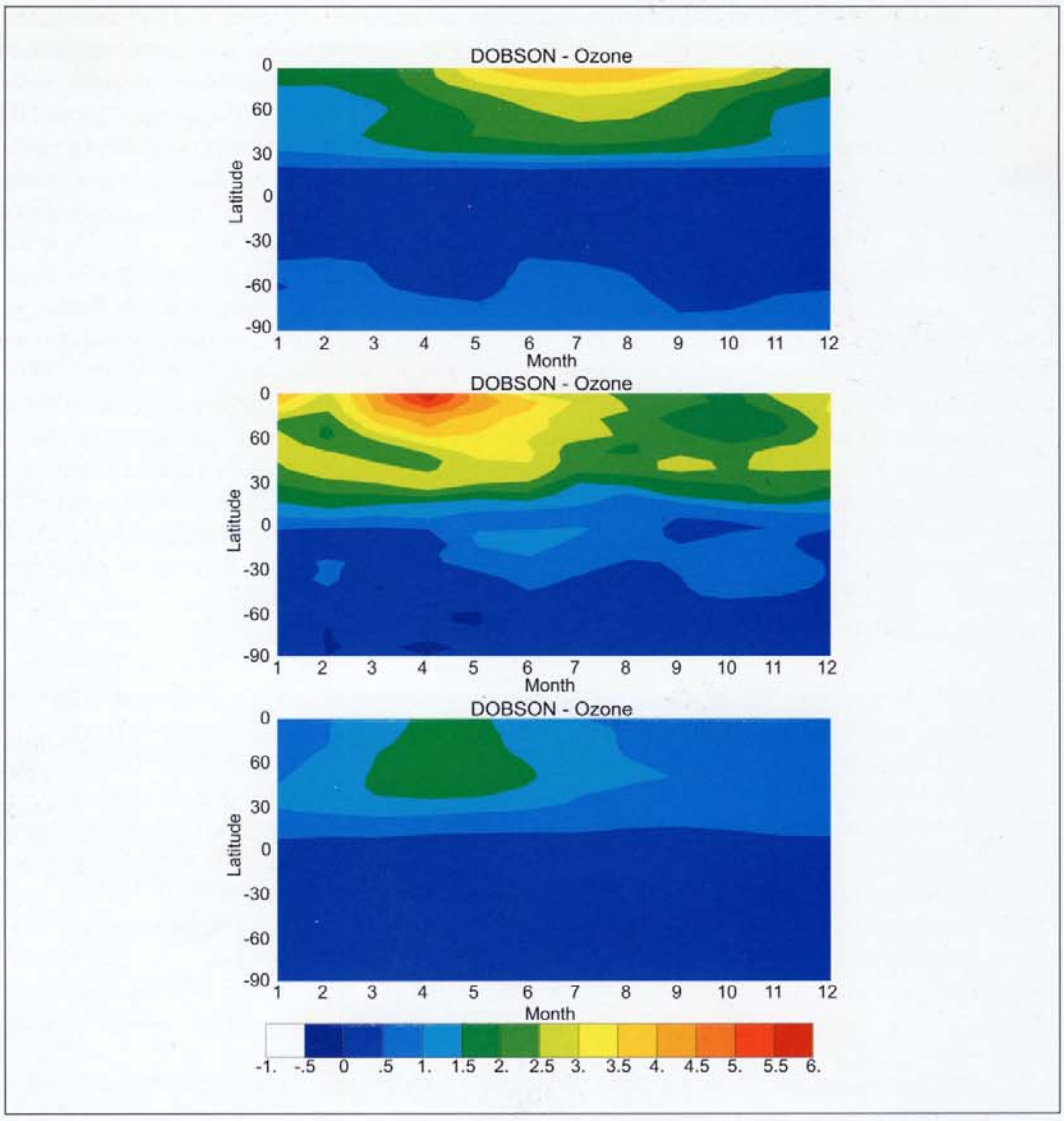

Figure 7.19 *Zonally averaged enhancement of tropospheric ozone column (Dobson units, DU) due to NO_x emissions from aircraft in 2015 in the University of l'Aquila (ULAQ) model (upper panel), the ECHAM/CHEM model (middle panel), and in the Oslo CTM-2 model (lower panel). Note that the plots are based on interpolated data and that the contour levels are the same in the three plots. The maximum values in the three computations are 4.07, 6.14, and 1.80 DU in the three panels from top to bottom. The minimum values are essentially zero in all three cases. The ECHAM and ULAQ results are integrals of O_3 changes from the surface up to 150 and 100 hPa, respectively. ECHAM/CHEM uses 39 levels, the ULAQ model uses 26 log-pressure levels from the ground to about 4 Pa with, and the CTM-2 model uses 19 levels between surface and 10 hPa. The vertical resolutions are 700 m, 2 km and 2.8 km near the tropopause height in the ECHAM, the CTM-2, and the ULAQ models, respectively. The horizontal resolution in the ULAQ (of University of l'Aquila) model is about 10° x 20°; the chemical scheme merges both tropospheric and stratospheric cycles; dynamics is taken from a low-resolution GCM. ECHAM/CHEM is a fully coupled chemistry-climate model; the results are based on multi-year model simulations (20-yr). The Oslo CTM-2 model is a chemical transport model, which uses dynamic input of one year (1996) from simulations performed at ECMWF with T63, L19, and 3-hour resolution. [T. Berntsen, M. Dameris, F. Mager, and G. Pitari, personal communication, 2001].*

most other similar models. The chemical scheme in the ULAQ model merges both tropospheric and stratospheric cycles and dynamics. The model might underestimate convective upwelling and this may explain why summer O_3 changes are relatively large in this model compared to the two others. The underestimate of O_3 perturbations in the Oslo model may partially be caused by an underestimate of wet scavenging by large scale precipitation, and larger NO_x emissions over Asia. Both effects enhance the background NO_x levels and reduce the O_3 production rate. More efficient convection, transporting O_3 precursors up from the ground and O_3 down to the surface (where it undergoes surface deposition) together with possibly some missing O_3 chemical production in the lower stratosphere, may also contribute to the differences.

These models do not account for the local conversion of emitted NO_x in the exhaust plumes into nitric acid. This conversion reduces the amount of large-scale ozone generation by about 10-30% [Karol et al., 2000; Kraabøl and Stordal, 2000; Kraabøl et al., 2000a, 2000b; Meijer et al., 1997; Moulik and Milford, 1999; Petry et al., 1998; Valks and Velders, 1999].

Future nitrogen oxides and ozone changes in the atmosphere due to growing aircraft NO_x emissions are slightly mitigated by an enhanced hydrological cycle and increased oxidation capacity of the atmosphere in the future climate [Grewe et al., 1999; Johnson et al., 1999; Stevenson et al., 2000].

Reduced Methane Lifetime

The emissions of NO_x affect the concentration of hydroxyl radicals (OH), which is the primary oxidising agent in the atmosphere. An increase in OH concentrations causes reductions of the chemical lifetime of methane (CH_4) in the atmosphere. An OH increase of up to 30% or more has been computed for aviation emissions in summer [see Schumann et al., 2000a]. Increased emissions of NO_x affect the partitioning within the HO_x family in favour of OH through the reaction:

$$HO_2 + NO \rightarrow OH + NO_2$$

NO_x emissions also affect OH levels through production of O_3, thereby increasing the primary production of HO_x radicals:

$$O_3 + h\nu \rightarrow O(^1D) + O_2$$

$$O(^1D) + H_2O \rightarrow 2\ OH$$

For these reasons, additional NO_x from aircraft is expected to cause local increases in OH radicals. Such radicals are short-lived and react with CO both in warm and cold air masses; they react also with CH_4 but essentially only in warm air. In the cold upper troposphere the increased OH radicals reduce the concentration of CO at flight levels, but reduce CH_4 only slightly. The lifetime of CO of approximately 2 months is longer than the time scale for vertical mixing in the troposphere. Therefore, the CO reduction is felt also near the surface. Reduced CO abundance near the surface in warm air masses leaves more OH radicals from other sources to react with CH_4. This may be one explanation of how aircraft NO_x emissions could indirectly cause a reduction of CH_4. Moreover, the increase in O_3 due to aviation may provide an additional OH source and contribute to enhanced CH_4 reduction. The 3-D models predict stronger effects than earlier 2-D model studies, because of stronger downward mixing of CO [Fuglestvedt et al., 1996, 1999; IPCC, 1999].

The CH_4 concentration in 1992 has been estimated to be about 2% less than that in an atmosphere without aircraft [IPCC, 1999]. For the 2015 emissions AEROCHEM II found reductions of methane lifetime by 1.2% and 0.6% in two models, which is significantly less than what was expected by 6 CTMs in IPCC [1999] (average of 2.5%) (see papers submitted 2001 for a special AEROCHEM issue to appear in Meteorologische Zeitschrift). For comparison, scenario calculations indicate that the CH_4 lifetime in the atmosphere has increased by about 25-30% during the past 150 years to a current value of about 7.9 years [Lelieveld et al., 1998]. The CH_4 lifetimes are computed to lengthen by 7-12% between 1990 and 2100 due to all anthropogenic emissions for fixed climate; however, when climate change is included, the lifetime would fall by 0-5% [Stevenson et al., 2000]. Hence, the magnitude of the aviation NO_x impact on methane is still very uncertain. The aircraft-induced reduction of CH_4 concentration is much smaller than the observed overall 2.5-fold increase since pre-industrial times. Reductions in CH_4 tend to cool the surface of the Earth.

7.3.5 Aircraft-induced effects on climate

The increased climate forcing caused by growing subsonic aircraft emissions, previously assessed in the special report of IPCC [1999] on "Aviation and the Global Atmosphere", see Figure 7.1, still remain of considerable concern for the future. A number of more recent studies broadly support the conclusions of IPCC [1999], these are outlined below. Generally it is recognised that the influence of aircraft on the Earth's temperature change is too small to detect and will likely remain undetected for at least the next decade. This makes it impossible to verify our results or predictions at present. It is also difficult to separate the aircraft-only signal from the effects of other anthropogenic changes in ozone and carbon dioxide.

Methodology

Radiative forcing has been widely used in the past to compare the magnitudes of different climate effects [Forster et al., 1997; Haywood and Boucher, 2000; IPCC, 2001]. However, there is some discussion as to whether it is an appropriate tool for understanding of the response of the climate system to non-uniform regional forcings, such as that from ozone and contrails.

It has been found in a number of studies with coupled ocean atmosphere GCMs [Bintanja et al., 1996; Christiansen, 1999; Hansen et al., 1997; Stuber et al., 2001], that the climate sensitivity (the ratio between globally averaged surface temperature change and radiative forcing) is different for ozone and carbon dioxide changes. It is further known that the regional scale of an applied forcing influences the magnitude of response [Forster et al., 2000; Ponater et al., 1999]. These factors would argue against the use of radiative forcing as an appropriate tool in the study of aircraft effects. However, as there is a larger difference between the climate sensitivity of different models, with the same forcing, than between the climate sensitivity for different forcings, in the same model, Forster et al. [1999] argue that until discrepancies between different GCM responses can be resolved radiative forcing still provides the best estimate of climate change. As the expected impact of aircraft is relatively small, very long runs of numerical models are needed in order to obtain a statistically significant result [Ponater et al., 1999]; again this suggests that radiative forcing is presently the more appropriate tool, at least for the first order global comparison of different effects.

The perturbation in radiatively active gases and particles could alter the temperature distribution and thereby the dynamics of the atmosphere. Pitari and Mancini [2001] show that

changes in the composition of the stratosphere by supersonic aircraft emissions could have a larger impact on the ozone distribution by changes in the dynamics than by the chemical reactions alone. They find that the change in radiative forcing is strongly reduced as a result of changes in the dynamics.

The impact of present subsonic aviation on short wave RF, due to changes in stratospheric sulphate aerosols, is small (order –0.003 Wm^{-2}) as confirmed recently by Pitari et al. [2001b].

Carbon Dioxide

Using a linear response model, Sausen and Schumann [2000] calculated the response of the global mean atmospheric carbon dioxide (CO_2) concentration and surface temperature to several aviation CO_2 emission scenarios, which are based on reported fuel consumption for the past, and IPCC scenarios for the future. Up to 2000, the accumulation of CO_2 emissions by aircraft have contributed to climate change through an increase in radiative forcing by about 0.028 Wm^{-2} in this model, or 1.9% of the radiative forcing from all anthropogenic CO_2 emissions (about 1.46 Wm^{-2} [IPCC, 2001]). Their reference scenario, which assumed a three-fold increase in aviation fuel consumption by 2050 and an annual increase of 1% thereafter, led to a surface temperature change of 0.05 K by 2100, agreeing with previous studies. They also estimated the effects of changes in NO_x emissions (further discussed below), finding a larger and more rapid surface temperature change for aircraft-induced ozone changes. Finally, they estimated the effects of using a proposed new combustor technology, which reduces NO_x emissions at the expense of slightly increased fuel consumption. They found that this technology leads to a reduced temperature increase over the next century.

Ozone

Because of conversion of NO_x to less reactive compounds in the exhaust plume the amount of large-scale ozone generation is smaller by 10-30%. This has direct implication for the related radiative forcing. Models show a slightly smaller increase in ozone resulting from aviation NO_x emissions if greenhouse warming feedbacks are included in future climate predictions. The slightly smaller increase in tropospheric ozone per emitted mass of NO_x reduces the RF increase expected in future scenarios. New observations confirm that modern more efficient engines form contrails over a larger range of altitudes. However such differences may be considered small compared to the general level of uncertainty.

Recent calculations of RF due to changes in tropospheric O_3, found the contribution due to aviation to be less than 0.01 Wm^{-2} in the period 1980-1996 [Karlsdóttir et al., 2000; Myhre et al., 2000]. The aircraft fuel consumption increased from 129 to 188 Tg yr^{-1} during this period [IEA, 2000], implying a value of order 0.03-0.04 Wm^{-2} for the total aircraft effect in 2000, slightly more than the best estimate given in IPCC [1999].

Using the ECHAM4 GCM coupled to a mixed layer ocean model, Ponater et al. [1999] extended an earlier study of the effects of prescribed O_3 changes by Sausen et al. [1997]. Equilibrium experiments have been performed representing aircraft induced ozone changes for 1992 and 2015. In both cases a small but statistically significant climate change is found. The amplitude of the equilibrium surface temperature response is of a magnitude 0.06-0.09 K, comparable to that arising from aircraft CO_2 emissions. The temperature response has a characteristic pattern different from that for changes in well-mixed greenhouse gases. The

sensitivity to non-uniform ozone changes near the tropopause was found to be higher (up to a factor of 1.6) than for a uniform change of a greenhouse gas [Stuber et al., 2001].

Methane

Nitrogen oxide emissions from aircraft slightly reduce the present increase in methane, which is a greenhouse gas. As explained above model studies performed within AEROCHEM find this effect to be smaller than the previous estimates from IPCC [1999].

Water Vapour Emissions

There is evidence of stratospheric water vapour increases over the last twenty years [Oltmans et al., 2000]. Forster and Shine [1999] and Smith et al. [2001b] calculate that these changes may have led to a lower stratospheric cooling of roughly 1 K and a positive radiative forcing of about 0.2 Wm^{-2}. Tracer simulations [Danilin et al., 1998] suggest that aircraft emissions are not the source of the observed H_2O changes. Scaling their simulation results with the emission index of H_2O shows that the aircraft water vapour emission can account for at most 5% of the water vapour change. Using the calculations by Forster and Shine [1999], this gives an insignificant radiative forcing of less than 0.01 Wm^{-2}. The direct RF by H_2O emissions would be small (about 0.002 Wm^{-2} for a scenario of 2015) even if all aircraft would burn liquid hydrogen instead of kerosene [Marquart et al., 2001] (the relative change in H_2O concentration reaches 0.41%). While the current contribution of aircraft emissions to stratospheric water vapour change is small, far larger concentration changes and RF values would probably result from a large fleet of supersonic aircraft emitting water vapour directly into the stratosphere [IPCC, 1999].

Contrails

Contrails, similar to thin cirrus, reduce the amount of short wave radiation reaching the Earth (albedo effect) and also reduce the long-wave radiation leaving the Earth to space (greenhouse effect) [Meerkötter et al., 1999]. Contrails may therefore reduce the radiative heating at the surface whilst causing a warming of the whole atmosphere.

The RF by contrails was computed assuming the contrails to be geometrically and optically thin plane parallel homogeneous cirrus layers in a static atmosphere [Meerkötter et al., 1999; Minnis et al., 1999; Strauss et al., 1997]. Most of the studies performed so far do not consider geometrical effects from narrow contrails. Inhomogeneity effects may be large in natural cirrus [Kinne et al., 1997; Pomroy and Illingworth, 2000; Raschke et al., 1998], but were considered small for vertically thin cloud layers in the few studies addressing this issue [Schulz, 1998]. However, measurements of downward fluxes below contrails from aircraft [Kuhn, 1970] and at the Earth's surface [Sassen, 1997] revealed rather large reductions in downward shortwave flux in the shadow of individual contrails with little gain by infrared radiation. This might be a consequence of the narrow geometry of contrails, which has not yet been evaluated.

The computations reveal a positive RF at the top of the atmosphere during night and day at least in many cases with thin cirrus [Meerkötter et al., 1999]. Negative RF values occur for thick cirrus with optical depth above 10 or ice water contents above 10 g m^{-2} [Fortuin et al., 1995; Zhang et al., 1999]. Such large values are unlikely to occur in persistent contrails, in

which the optical depth is usually below 1 and the ice water content below 5 g m^{-2}. Negative RF values occur, even for thin cirrus, over dark and cold surfaces such as over the North Atlantic in winter [Meerkötter et al., 1999; Meyer et al., 2001].

The global mean RF computed by Minnis et al. [1999] were used for IPCC [1999]. The results imply a global mean RF of 0.02 Wm^{-2} in 1992, and 0.1 Wm^{-2} in 2050. The results depend strongly on the assumed values for cover (0.1% and 0.5% global mean cover for 1992 and 2050), optical thickness (0.3), and particle shape (hexagons). As mentioned in Section 7.3.2, recent studies indicate smaller optical thickness values over Europe (near 0.1) but seem to support values of order of 0.3 over the USA. A recent GCM study of Ponater et al. [2000, 2001], discussed next, shows variations in the cover and optical depth of contrails with latitude, altitude, and season, which may explain the observed differences in optical depth of contrails in various regions, see Figure 7.20.

With respect to climate change the role of line-shaped contrails are found to be smaller than in previous estimates. Ponater et al. [2001] computed the cover and optical properties of contrails using a parameterisation similar to those for cirrus clouds within a GCM, including the Schmidt-Appleman criterion. With respect to cover computations, the method is the same as that used in Sausen et al. [1998], but the present method uses the meteorological fields

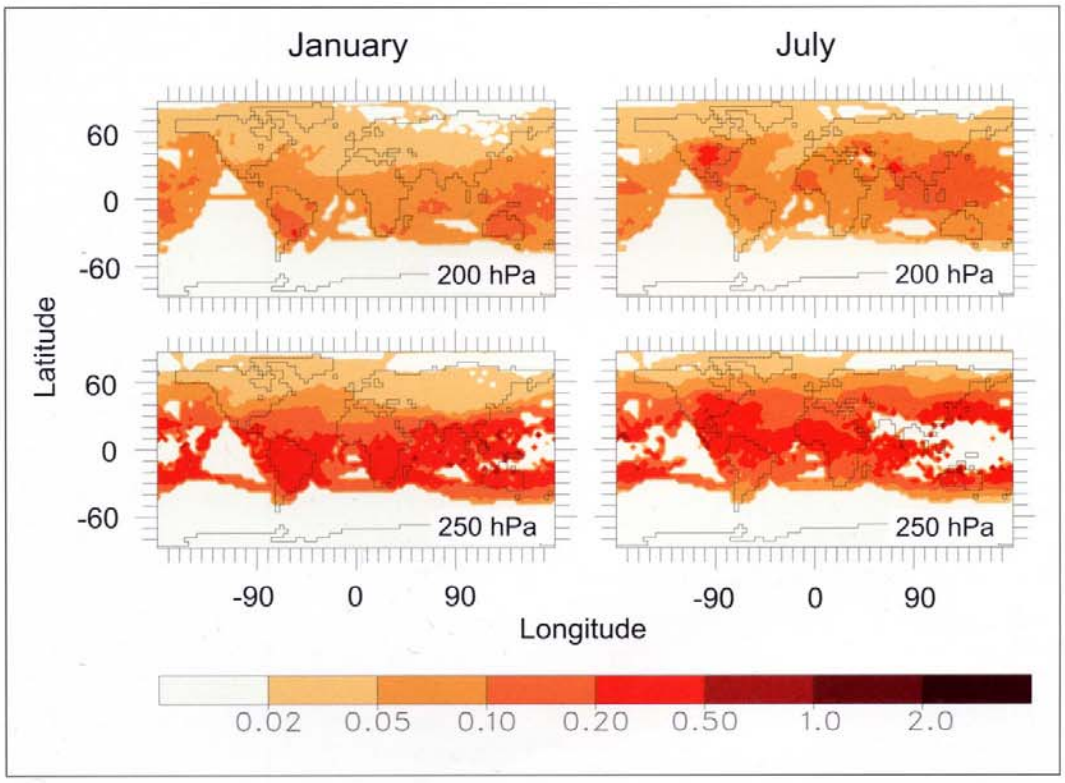

Figure 7.20 *Mean optical depth of contrails as computed with a contrail parameterisation in the global circulation model ECHAM, at 200 and 250 hPa pressure altitude and for January and July. Note that the optical depth is nondimensional and is computed at places where contrails exist, regardless of the amount of contrail cover [Ponater et al., 2001].*

computed by the global circulation model ECHAM, and also computes the ice water content and radiative properties of contrails. The time mean value of the contrail cover is found to be close to that computed by Sausen et al. [1998]. The values of optical depth (mean of 0.06 over Europe) is much smaller than those reported from local observations, and even smaller than the value (about 0.1) deduced by Meyer et al. [2001]. The RF of contrails resulting from the model experiments is substantially lower than estimated by Minnis et al. [1999]. One contribution to the disagreement arises from the smaller mean ice water content giving smaller optical depth in the climate model simulations. However, the largest part can be explained by a strong sensitivity of the contrail climate impact to a different mean altitude of the contrails and to a different extent of interference with natural high clouds. The computed RF values would have been computed to be even smaller when using the most recent cover results of Mannstein et al. [1999] and Meyer et al. [2001] instead of Bakan et al. [1994] for normalisation of computed contrail cover. As the model, like most GCMs, suffers from a cold bias at the extra-tropical tropopause, the consequences of systematic errors in simulated temperature and humidity needs to be investigated further. The same is true for an adequate representation of contrails-cirrus overlap and its influence on the contrail radiative impact in this, as well as in other models. However, the recent studies by Meyer et al. [2001] and Ponater et al. [2001] suggest that the RF by line-shaped contrails may be considerably smaller than the value reported in IPCC [1999]. Still, this does not account for the indirect effects of contrails and aerosols from aircraft on cirrus cloud changes.

For a regional additional 0.5% cirrus cloud cover, Strauss et al., [1997] calculated a regional surface temperature increase of the order 0.05 K. For 1% additional cirrus cloud cover with 0.33 optical depth in the solar range, a recent study with a global circulation model coupled to a mixed layer ocean model computed 0.43 K global warming at the surface, i.e., more than four times higher climate sensitivity [Rind et al., 2000]. However, this study makes a series of assumptions about the optical properties of the aircraft induced cirrus that need to be verified. First tests with an aerosol dependent cirrus model in a GCM show that different treatments of ice nucleation in the model result in longwave cloud forcing changes of 4 Wm^{-2}; this shows that the aerosol/cirrus interactions are important, but the quantitative effects need to be studied further [Lohmann, 2000].

Preliminary plans are discussed to reconsider the build and operation of supersonic aircraft by the European aviation industry. Moreover, American aircraft manufacturers are also considering building a new large aircraft which flies slightly faster (nearly at Mach 1) and higher than the present fleet of subsonic aircraft. Flying higher could be environmentally acceptable because of reduced contrail formation if one can conclusively show that the chemical effects of the emissions are of minor importance and if the amount of fuel consumption is smaller than for present aircraft. The environmental effects of such plans need to be assessed carefully before final decisions are taken to build such aircraft.

Acknowledgements. The authors thank M. Dameris, K. Gierens, V. Grewe, B. Kärcher, A. Kiendler, F. Mager, S. Marquart, R. Meyer, A. Petzold, G. Pitari, M. Ponater, F. Schröder, K.-H. Wohlfrom, and H. Ziereis, for valuable input and comments on draft versions of this review which improved the paper considerably. The authors also thank the reviewers for helpful comments improving the manuscript. In particular the authors gratefully acknowledge the very helpful contributions to this chapter by David W. Fahey during the final review meeting.

Table 7.1 *Atmospheric Research Projects on Aviation Impact*

Acronym	Programme Title	Period	Fund. Agency	Reference
AEROCHEM I and II	Modelling of the Impact on Ozone and Other Chemical Compounds in the Atmosphere from Airplane Emissions	1994-1998	EC	Isaksen [1998]; 2000]
AERO-CONTRAIL	Formation processes and radiative properties of particles in aircraft wakes	1994-1997	EC	Mirabel [1998]
AERONOX	The Impact of NO_x Emissions From Aircraft Upon the Atmosphere at Flight Altitudes 8-15 km	1992-1994	EC	Schumann [1995, 1997a]
CARIBIC	Civil Aircraft for Remote Sensing and *In situ* Measurements in the Troposphere and lower Stratosphere Based on the Instrumentation Container Concept	1996-1999	EC	Brenninkmeijer et al. [1999]
CHEMICON	Chemistry and Microphysics of Contrail Formation	1998-2000	EC	Zellner [2000]
CLOUDMAP I, II	Cirrus and contrail cloud-top maps from satellites for weather forecasting and climate change analysis.	1997-2003	EC	http://www.ge.ucl.ac.uk/research/CLOUDMAP.html
CRYOPLANE	Liquid hydrogen fuelled aircraft-system analysis	2000-2003	EC	Klug and Ponater [2000]
EULINOX	European Lightning NO_x Experiment	1998-2000	EC	Höller and Schumann [2000]
GMI	Global Modelling Initiative	1995-2000	NASA	Kinnison et al. [2001]
INCA	Inter-hemispheric differences in cirrus properties from anthropogenic emissions, http://www.pa.op.dlr.de/inca/	2000-2002	EC	Ström et al. [2000]
LOWNOX III	Low Emission Technology Program, Phase III, see http://dbs.cordis.lu/, http://www.aero-net.org/	1996-2001	EC	L. Verdier, SNECMA
METRIC	Metrics of Climate Change	2000-2003	EC	R. Sausen, Oberpfaffenhofen
MOZAIC I, II, III	Measurement of Ozone by Airbus In-Service Aircraft	1993-2003	EC	Marenco et al. [1998]
NOXAR	Nitrogen Oxides and Ozone along Air Routes	1994-1997	BAZL, Swiss Fed. Office for Aviation	Brunner et al. [1998]
PARTEMIS	Measurement and Prediction of Aerosols and Gaseous Precursors From Turbine Engines	2000-2003	EC	C. Wilson, Pyestock
PAZI	Particles from aircraft engines and their influence on contrails, cirrus and climate (Partikel and Zirren)	2000-2003	HGF, DLR, AWI, FZJ, FZK	http://www.pa.op.dlr.de/pazi/
POLINAT 1, 2	Pollution From Aircraft Emissions in the North Atlantic Flight Corridor	1994-1998	EC	Schumann et al. [2000a]
SNIF	Subsonic Assessment Near Field Interactions Flight	1996-1998	NASA	Hunton et al., [2000]
SIL	Pollutants from Air Traffic (Schadstoffe in der Luftfahrt)	1992-1997	BMBF, DLR	Schumann et al. [1997]
SONEX	Subsonic Assessment Ozone and Nitrogen Oxides Experiment	1996-1998	NASA	Thompson et al. [2000]
STREAM I, II, III	Stratosphere-Troposphere Experiments by Aircraft Measurements	1994-1998	EC	Lelieveld et al. [1996, 1999b, 2000]
SUCCESS	Subsonic aircraft: Contrail and cloud effects special study	1996-1997	NASA	Toon and Miake-Lye [1998]
SULFUR 1-7	Fuel sulphur impact on contrails and aerosols	1994-1999	DLR, DFG, BMBF	Schumann et al. [1997, 2001]
TOPOZ II	Towards the Prediction of Stratospheric Ozone, II	1998-1999	EC	http://www.atm.ox.ac.uk/TOPOZII/
TRADEOFF	Aircraft emissions: Contributions of various climate compounds to changes in composition and radiative forcing - trade-off to reduce atmospheric impact	2000-2003	EC	I. Isaksen, Oslo
UTLS OZONE	Laboratory studies of the heterogeneous interaction of pollutants from aircraft – HNO_3, H_2O and soot aerosols	1999-2002	NERC	R.A. Cox, Cambridge
UTLS OZONE	Development of Scientific Instrumentation for Commercial Aircraft	1999-2000	NERC	R. Jones, Cambridge

Table 7.2 *Consumed or emitted species, mean emission indices (mass of emissions per unit mass of burned fuel, for the fleet of aircraft in 2000) total emission rates due to aviation and for comparison emission rates from other sources (adapted for 2000 from IPCC [1999]. Fuel consumption is based on extrapolated data of the International Energy Agency until 1998 [IEA, 2000] and data of the Department of Energy of the USA (http://www.eia.doe.gov/emeu/international/petroleu.html).*

Species	Emission index, g/kg (ranges)	Emission rate (2000) in Tg yr^{-1}	Comparable emission rate, Tg yr^{-1}	Comparable emission source
Kerosene		220	3140	Total petrol production
CO_2	3160	700	26000-30000	Total anthropogenic CO_2 emissions
H_2O	1230	270	45	Methane oxidation in the stratosphere
			525000	Evaporation of H_2O from Earth's surface
NO_x	14	3	2.9±1.4	Stratospheric sources
			7-80	Lightning
			90±35	Total anthropogenic source
Soot	0.04 (0.01-0.06)	0.009	12	Combustion of fossil fuels and biomass
SO_2	0.8 (0.6-1.0)	0.18	130	Total source from burning fossil fuels
			20-100	Natural sources
			5.4, 8.0	Non-eruptive, eruptive volcanoes
CO	4 (2-6)	0.	1500	Total anthropogenic sources
HC	0.1 (0.001-1.0)	0.02	90	Total anthropogenic sources

Table 7.3 *Equivalent emission indices for condensable gases (excluding H_2O), soot and hydroxyl radicals emitted by aircraft engines or formed in the very young exhaust plume.*

Species	Emission index ranges (g/kg) [A]	Source
Soot	0.04 (0.01-0.1) [B]	Fuel carbon
H_2SO_4	0.04 (0.01-0.1) [C]	Fuel sulphur $SO_2 + OH$, $SO_2 + O$
HNO_3, [D]	0.02-0.3	Fuel- and air-nitrogen passed through combustor, NO_2+OH
OH	0.1-0.5[E]	Combustion
Low volatility hydrocarbons	≈0.01-0.02 [F]	Fuel carbon
Volatile aerosol particles	0.0065-0.05 [G]	Condensable gases

[A] Equivalent emission index

[B] Modern engines have a soot emission index of about 0.01 g soot per kg fuel

[C] For a mean fuel sulphur content of 400 μg/g and a measured efficiency ε=0.033 for fuel sulphur conversion to H_2SO_4. Commonly used fuel sulphur content values range from 10 to 1000 μg/g (upper limit 3000 μg/g).

[D] Condensable only in very cold, lower stratosphere (see text). (T≤200 K)

[E] Inferred from measurements with chemical plume models.

[F] Inferred from measurements (see text) and from Kärcher et al. [2000]. Very uncertain.

[G] Taking 10^{16}-10^{17} volatile particles (diameter 5 nm) and assuming a specific weight of 1 g/cm^3. Very uncertain.

Table 7.4 *Global nitrogen oxide sources in Tg(N)/yr (Lee et al., [1997b] including new data for 2000 aviation) and their estimated contributions to concentration change in the upper troposphere at 30-60°N.*

Source	**Source Rate in Tg(N)/year**	**NO_x concentration contribution at 30-60°N, 9-11 km altitude**
Aircraft engines	0.9 (0.7-1.0)	30%
Lightning	5 (2-20)	20%
Industry and Surface Traffic	22 (13-31)	30%
Biomass Burning	8 (3-15)	10%
Soil	7 (4-12)	5%
$N_2O + O \rightarrow 2\ NO$ (Stratosphere)	0.6 (0.4-1.0)	5%